Fundamentals and Recent Progress in the Flow of Water-Soluble Polymers in Porous Media for Enhanced Oil Recovery

Mirzaie Yegane, M.; Boukany, P.; Zitha, P.L.J.

DOI
10.3390/en15228575

Publication date
2022

Document Version
Final published version

Published in
Energies

Citation (APA)
Mirzaie Yegane, M., Boukany, P., & Zitha, P. L. J. (2022). Fundamentals and Recent Progress in the Flow of Water-Soluble Polymers in Porous Media for Enhanced Oil Recovery. *Energies*, *15*(22), Article 8575. https://doi.org/10.3390/en15228575

energies

MDPI

Review

Fundamentals and Recent Progress in the Flow of Water-Soluble Polymers in Porous Media for Enhanced Oil Recovery

Mohsen Mirzaie Yegane [1,*], Pouyan E. Boukany [2] and Pacelli Zitha [1]

[1] Department of Geosciences and Engineering, Delft University of Technology, 2628 CN Delft, The Netherlands
[2] Department of Chemical Engineering, Delft University of Technology, 2629 HZ Delft, The Netherlands
* Correspondence: m.mirzaieyegane@tudelft.nl; Tel.: +31-15-27-85139

Abstract: Due to increased energy demand, it is vital to enhance the recovery from existing oilfields. Polymer flooding is the most frequently used chemical enhanced oil recovery (cEOR) method in field applications that increases the oil sweep and displacement efficiencies. In recent years, there has been growing interest to assess the use of polymer flooding in an increasing number of field applications. This is due to the improved properties of polymers at high-salinity and high-temperature conditions and an increased understanding of the transport mechanisms of water-soluble polymers in porous media. In this review, we present an overview of the latest research into the application of polymers for cEOR, including mechanisms of oil recovery improvement and transport mechanisms in porous media. We focus on the recent advances that have been made to develop polymers that are suitable for high-salinity and high-temperature conditions and shed light on new insights into the flow of water-soluble polymers in porous media. We observed that the viscoelastic behavior of polymers in porous media (e.g., shear thickening and elastic turbulence) is the most recently debated polymer flow mechanism in cEOR applications. Moreover, advanced water-soluble polymers, including hydrophobically modified polymers and salt- and temperature-tolerant modified polyacrylamides, have shown promising results at high-salinity and high-temperature conditions.

Keywords: chemical enhanced oil recovery (cEOR); polymer; nanoparticles; high salinity; high temperature

Citation: Mirzaie Yegane, M.; Boukany, P.E.; Zitha, P. Fundamentals and Recent Progress in the Flow of Water-Soluble Polymers in Porous Media for Enhanced Oil Recovery. *Energies* **2022**, *15*, 8575. https://doi.org/10.3390/en15228575

Academic Editor: Dmitriy A. Martyushev

Received: 24 October 2022
Accepted: 12 November 2022
Published: 16 November 2022

1. Introduction

With the increasing world population, meeting the growing energy demand in a safe and environmentally responsible manner is a vital challenge. In 2040, oil and natural gas will still account for over 50% of the world's energy consumption [1], yet the contribution of renewable energy resources appears to be inadequate in meeting the rising energy demand. Due to increased energy demand, it is imperative to maximize the recovery from existing oilfields. The recovery factor of mature oilfields is nearly 30% [2,3], which means a large proportion of "original oil in place" (OOIP) is left behind in the subsurface. This increases the potential for enhanced oil recovery (EOR) methods. These include thermal, gas, and chemical methods [4–9]. The latter is also known as chemical enhanced oil recovery (cEOR).

Polymer flooding is a tertiary oil recovery technique, typically employed after water flooding, where a small amount of a water-soluble polymer is added to water (brine) to increase its viscosity. The presence of polymer macromolecules in water reduces its mobility and consequently reduces the fractional flow of water. This in turn helps with the reduction of viscous fingering and increases the volumetric sweep efficiency [4]. The concept of polymer injection was first established by Pye [10] and Sandiford [11] in 1964, when they observed that water mobility was reduced and oil recovery was improved by water-soluble polymers; these included the extended family of acrylamide polymers. Several pilots and field applications were then reported in the USA during the 1970s and 1980s [12–16] and, since the mid-1990s, polymer flooding has also been implemented in China with success [17–20]. Several review articles have discussed the application of conventional

cEOR polymers for full-scale polymer floods and the knowledge and learning related to the logistics of field execution, process development, and key concepts for successful implementation of the technology [12,13,21–30].

In the past decade, the application of water-soluble polymers has been considered for use in an increasing number of field projects [31]. This is because of (a) recent improvements in the properties of polymers at high-salinity and high-temperature conditions compared with conventional cEOR polymers and (b) an improved understanding of mechanisms behind water-soluble polymers' flow in porous media.

Partially hydrolyzed polyacrylamide (known as HPAM) and xanthan gum, which are the two most common polymers used in field applications, have shown challenges at high salinities and temperatures. At high salinities, electrostatic repulsions between the negative charges of the carboxylate groups present along the HPAM backbone can be screened due to the presence of di- or monovalent cations, which leads to a reduction in the viscosity [32–34]. This effect is worsened by an increase in temperature because the acrylamide monomers are further hydrolyzed [35]. Even though the xanthan gum is more resistant to high salinities and temperatures, it is very susceptible to bacterial degradation [36,37] and its solution contains some cellular debris that can cause pore clogging [32]. Recently, several researchers have focused on synthesizing water-soluble polymers with improved rheological properties at high salinities and temperatures [38–42].

Furthermore, in recent years, several studies have shed light on the flow mechanisms of water-soluble polymers in porous media that are still the subject of debate among researchers. Several mechanisms have been discussed, among which are the anomalous shear-thickening behavior of synthetic polymers at high share rates and the reduction of residual oil saturation due to the viscoelastic properties of synthetic polymers [43–47].

In light of these developments, a comprehensive study is needed to address the recent progress in the flow of water-soluble polymers in porous media and to highlight any remaining challenges. The objective of this review is to revisit the fundamentals of polymer flow in porous media and to present the recent progress. There have been several reviews over the past three years that discuss the application of polymers for enhanced oil recovery [23,24,30,48–50]. In this review, we focus on the development of advanced polymers for high-salinity and high-temperature conditions and shed light on new insights into the flow mechanisms of water-soluble polymers in porous media.

An overview of this paper is given in Figure 1. Firstly, we discuss the oil recovery improvement mechanisms due to the polymer macromolecules present in water. Thereafter, the experimental, analytical, and numerical approaches to study polymer rheology and retention in porous media are discussed. In particular, several theoretical and experimental observations are presented to explain the anomalous shear-thickening behavior of synthetic polymers in porous media. Furthermore, a critical overview of the impact of several parameters on polymer transport mechanisms in porous media is given. Emphasis is placed on the impact of salinity and temperature on polymer performance in porous media, which hinders the applications of classic EOR polymers in field applications in harsh conditions. Therefore, we discuss the approaches that have focused on pushing the envelope for polymers towards high-salinity and high-temperature conditions. These include the hydrophobic modification of the conventional polymers or the incorporation of salt- and temperature-tolerant monomers to the HPAM backbone. Finally, a hybrid of polymer and nanoparticles is discussed as an innovative approach for improved viscosity and enhanced stability at high-salinity and high-temperature conditions.

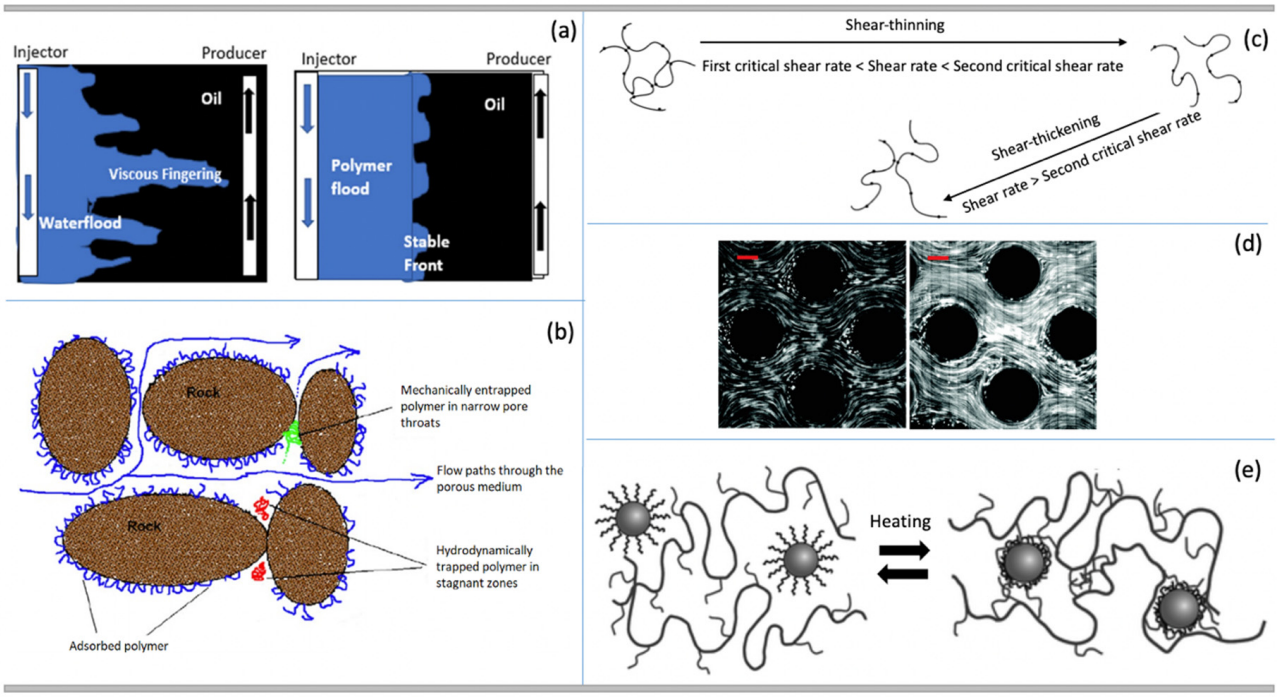

Figure 1. Oil recovery and transport mechanisms of water-soluble polymers, as will be discussed in this paper. (**a**) The decrease in water mobility due to the presence of polymer macromolecules in the water. Adapted with permission from [51]. (**b**) Polymer retention mechanisms in porous media. Adapted with permission from [52]. (**c**) Polymer rheology in porous media. Adapted with permission from [53]. (**d**) Shear-thickening behavior of polymers caused by elastic instabilities. Adapted with permission from [54]. (**e**) Improved rheological properties in harsh conditions by dispersions composed of a hybrid of nanoparticles and water-soluble thermo-responsive polymers. Adapted with permission from [55].

2. Polymer Flooding Mechanisms

2.1. Mobility Control

During water flooding, the front of the water moves more easily than the oil. The stability of the front depends on the balance of forces (e.g., gravity, capillary, and viscous forces, and dispersion) on the interface. When the destabilizing forces (e.g., viscous forces) are superior to the stabilizing forces (e.g., the dispersive and capillary forces), the microscopic perturbations, which are a result of small-scale heterogeneities, cause the formation of tongues of water at the interface, a phenomenon known as viscous fingering (see Figure 1a). This results in the bypassing of the oil and thus an early breakthrough of water followed by a long period of two-phase production.

It is conventionally believed that the oil recovery improvement observed in polymer flooding can be attributed to the concept of the mobility ratio [4,52,56], as defined by Equation (1):

$$M = \frac{\lambda_w}{\lambda_o} = \frac{k^e_{rw}\mu_o}{k^e_{ro}\mu_w} \quad (1)$$

where λ, k^e_r, and μ are the mobility, endpoint relative permeability, and viscosity, respectively, and where the subscripts o and w refer to oil and water, respectively. When the mobility ratio (M) is unfavorable (i.e., $M > 1$), there is a macroscopic sweep inefficiency that triggers an early breakthrough of water. The presence of polymer macromolecules in the water increases the volumetric sweep efficiency of the system. This is achieved through two mechanisms: (a) by reducing the drive water mobility and (b) by the reduction in disproportionate permeability.

Increasing the drive water viscosity reduces M to values lower than 1 (i.e., $M < 1$). As a result, the fractional flow of water is reduced and the fractional flow curve shifts rightward. Consequently, the average water saturation increases. This leads to a piston-like displacement of the oil (i.e., more oil is displaced). Drive water mobility can also be reduced due to polymer retention in porous media. Doda [57] showed that the reduction of water relative permeability because of polymer blockage in porous media reduces the mobility ratio.

The reduction in disproportionate permeability means that the water relative permeability is significantly reduced, while there is a minimum decrease in the oil relative permeability [58,59]. To achieve this, a crosslinking polymer is injected that propagates deep into the reservoir where it forms a gel. This can substantially reduce the permeability of thief zones and improve the vertical sweep efficiency. As a result, the drive water in the oil-bearing zones is diverted. The disproportionate permeability reduction results from the formation of an adsorbed layer of polymer on the pore wall and the segregation of the oil and water flow pathways [60–65]. The decrease in disproportionate permeability leads to a reduction in excessive water production while improving the oil recovery [66]. It should be pointed out that the importance of disproportionate permeability reduction is more significant for water control than for polymer flooding.

2.2. Effect of Polymer on Residual Oil Saturation

Until recently, it was believed that water-soluble polymers merely improved the macroscopic sweep efficiency with no impact on the microscopic displacement efficiency. However, an unexpected increase in the recovery factor from the Daqing oil field, of 13% of OOIP, generated questions about whether this could be explained by only considering the macroscopic efficiency [67]. Recent studies have suggested that polymer flooding may also improve the microscopic displacement efficiency [47,68]. This is accomplished by mobilizing and displacing the residual oil trapped by capillary forces and is attributed to the viscoelastic properties of the synthetic polymers used for cEOR. It takes place due to changes in the steady-state-flow profile and is due to the pulling effect, the thread formation, and the oil stripping [43].

During the flow of a viscoelastic polymer solution through the dead ends in porous media, normal stresses between oil and polymer solution are generated in addition to the shear stresses which exist due to long polymer chains. Therefore, polymer chains apply a larger force on the oil droplets and grab their upper part. As a result, the oil droplets are detached from the surface of dead ends [69]. It is argued that an increase in the level of elasticity of polymer reduces the amount of oil droplets trapped in the dead ends [70].

When the polymer molecules flow downstream, they aggregate with oil droplets that are trapped by capillary forces. As a result, they are likely to pull the oil droplets out into oil columns forming oil threads. Due to high interfacial tension between oil droplets and polymer molecules, the oil column will be destabilized and break down into smaller droplets. These smaller droplets can then become re-entrapped by capillary forces. The use of elastic polymers is reported as a method to avoid this situation, as the normal stresses stabilize the oil thread [71].

The stripping effect refers to the movement of the adsorbed oil layer along the surface in oil-wet rocks. Near the capillary wall, the velocity gradient of a non-Newtonian fluid, such as a polymer solution, is larger than that of a Newtonian fluid, such as water [72]. As a result, when flowing near the capillary wall, the polymer solution exerts a greater force than water does, which then induces the movement of oil droplets [73]. Xie et al. [74] argued that the oscillation induced by the viscoelastic memory effect is the main reason for the recovery of nonwetting fluids by using a viscoelastic polymer solution [75].

Clarke et al. [46] showed a mechanism of flow fluctuations at low Reynolds numbers as a result of the flow of viscoelastic polymer solutions in porous media. They argued that these fluctuations in the flow explain both the enhanced capillary-desaturation curves and the observation of apparent flow thickening (this will be discussed in more detail

in Section 3.1). As a result of fluctuations in the flow, fluctuating pressure fields are generated that destabilize the trapped oil drops, or ganglia, and thus improve the oil recovery. Vermolen et al. [45] reported that for crude oil of high viscosity (~300 cP), no additional oil was recovered due to polymer viscoelasticity (even with increases in the polymer solution viscosity and flow rate), whereas for crude oil of low viscosity (~9 cP) additional oil was recovered upon increasing the viscosity and/or flow rate of the polymer of high elasticity.

Erincik et al. [76] performed a series of core-flood experiments in which the core was first waterflooded, followed by a viscous-glycerin flood, a low-salinity polymer flood, and a high-salinity polymer flood with the same viscosity. The low-salinity polymer flooding was performed at high Deborah numbers (see Section 3.1 for the definition of the Deborah number), whereas the high-salinity polymer flooding was performed at low Deborah numbers. The authors found that the low-salinity polymer flooding led to the reduction of residual oil saturation. However, the high-salinity polymer flooding unexpectedly resulted in a further reduction of the residual oil saturation. This was attributed to the relatively high-pressure gradients that could mobilize the oil bank, even though the capillary numbers were lower than the critical capillary number. Qi et al. [77] observed an average residual-oil reduction of 5% OOIP during HPAM polymer floods for Deborah numbers ranging from 0.6 to 25.

3. Polymer Rheology in Porous Media

3.1. Polymer Viscoelasticity in Porous Media

The flow of polymer solution in the microscopic structures of a porous medium is much more complex than the flow in the well-defined geometries of a classical rotational rheometer [52]. HPAM is known to show viscoelastic behavior in porous media, meaning that the HPAM solution behaves as a liquid and a solid simultaneously at certain shear rates. This viscoelastic behavior for HPAM is most likely to be observed at high polymer molecular weights and high concentrations. When the polymer solution flows into the pores, it is forced to change its speed so it can maintain a fixed volumetric rate. This results in the formation of extensional forces along the flow path near the pore walls while the polymer molecules are also under shear forces [49].

To characterize the viscoelastic properties of a polymer solution at various flow geometries, dimensionless numbers such as the Weissenberg number (*Wi*) and the Deborah number (*De*) have been used [78]. *Wi*, which is the product of relaxation time and strain rate, describes the non-isotropic arrangement of the polymer under shear stress. Hence, it provides insight into the mechanical properties of the fluid and quantifies its elasticity. For a Weissenberg number equal to zero, the fluid only shows viscous behavior, while at Weissenberg numbers higher than zero the fluid shows viscoelastic behavior. *De* is the ratio of relaxation time to the characteristic flow time and allows for quantification of the elastic strain. For Deborah numbers lower than 1, the polymer solution behaves like a viscous liquid, whereas for $De > 1$ it shows elastic characteristics as well [74,79].

In the literature, the flow behaviors that are related to the viscoelastic nature of a polymer solution in porous media are classified as shear-thinning and shear-thickening. For increasing shear rates, the apparent viscosity of polymer solutions versus the shear rate in porous media exhibits three main regions. At low shear rates, the polymer viscosity is independent of the shear rate (Newtonian behavior). Above a critical shear rate, the polymer viscosity decreases with an increasing shear rate because of the reduction in the number of interchain associations (shear-thinning or pseudo-plastic behavior). Finally, above a second critical shear rate, the polymer viscosity increases with the shear rate due to the stretching of the individual chains, which generates interchain bonding by coagulation (shear-thickening or dilatant behavior) (see Figure 1c) [6].

The shear-thickening behavior of polymer solutions has been investigated by flow experiments in a capillary as a very simple model porous media [80,81]. During the flow through capillaries, polymer solutions experience both shear stresses and extensional

stresses, the latter being essentially confined to the entry and exit zones of the capillary. Figure 2 compares the shear viscosity, measured by a rheometer, and the apparent viscosities in capillaries with varying lengths for an HPAM solution [82]. Below the second critical shear rate, the apparent and shear viscosities are identical. However, above this shear rate, high-pressure drops are observed in the capillaries, which results in the deviation of the apparent viscosity from the shear viscosity. The observed pressure drops can be expressed as a sum of three elements: (1) pressure drop at the entry, (2) pressure drop at the exit, and (3) pressure drop caused by the polymer friction with the wall. In capillaries with equal diameter, pressure drops at the entry and exit are almost equal and are independent of the capillary length, while the pressure drop due to the polymer friction with the wall increases with capillary length [83]. This results in an increase in apparent viscosity because the entry and exit effects become more significant as the length to radius ratio (l/r) decreases [84].

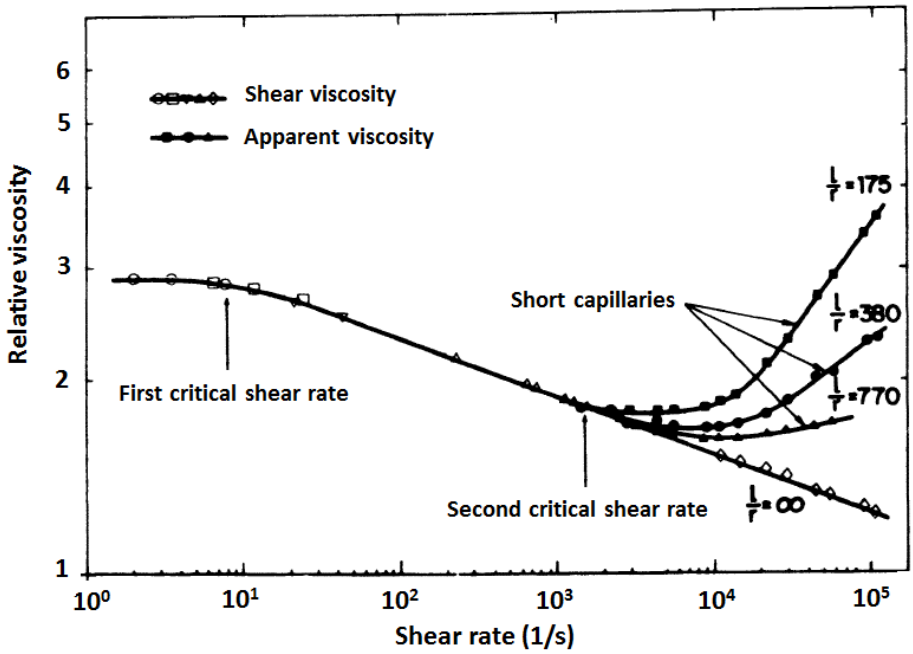

Figure 2. Comparison of shear and apparent viscosities in capillaries with different lengths. The experiments were performed at 30 °C with 0.034 wt% HPAM dissolved in a brine containing 2 wt% NaCl (1 wt% = 10,000 ppm). The radius (r) of the capillary was 1 mm and the length (l) varied. Adapted with permission from [82].

The exact mechanism of shear-thickening behavior in porous media has been a subject of much research and debate among researchers [44,85–89]. Several studies have demonstrated that the presence of extensional flow (also referred to as elongational flow) leads to a shear-thickening behavior [34,90–93]. Nonetheless, there is no consensus about the mechanism responsible for the extensional flow of polymer solutions in porous media. There are two difficulties in describing polymer flow through porous media: (1) the topological complexity of the pore network and the geometric complexity of the pore space and (2) the complex behavior of polymer molecules in extensional flows.

The first of the issues was studied by using simplified geometries such as (converging–diverging) capillaries to isolate the effects of the extensional flow [90,92,93] and the second was addressed in more recent studies using microfluidic devices that enabled simultaneous measurements of the apparent viscosity and the visualization of the polymer deformations due to extensional flows [54]. Here, we present the three main theories found in the literature that justify the increase in the viscosity of polymer solutions at high flow rates: (a) the coil–stretch theory, (b) the transient network theory, and (c) the presence of elastic flow instabilities.

In the coil–stretch theory, as De Gennes [94] predicted, the randomly coiled polymers will become fully extended at a critical strain rate ($\dot{\varepsilon_c}$) larger than the rate of relaxation and the coil–stretch transition will occur. This is the same as a Weissenberg number more than 1. However, a theoretical calculation based on the generalized Zimm model [95] and a numerical calculation by Larson and Magda [96] have shown that the commencement of the coil–stretch transition occurs when $Wi > 0.5$. Notably, single molecule experiments (by the DNA visualization) combined with microfluidics were used to verify the onset of the coil–stretch transition through flow at $Wi > 0.5$ [97–99].

In the transient network theory, the shear-thickening behavior of polymer solutions is related to the formation of transient networks of polymer chains. Such transient networks exist when entanglements among polymer chains become mechanically effective (i.e., both ends of a chain are incorporated in the network) at timescales shorter than the disentanglement time [100,101]. Shear-thickening effects were observed in (nearly) non-inertial flows for very dilute polymer solutions that would usually disfavor the transient network concept. However, if the polymer molecules are in a stretched state, the probability of forming locally transient networks will increase considerably.

The shear-thickening behavior has also been recently ascribed to the onset of an elastic instability at a negligible inertial effect, arising from the buildup of polymer-induced elastic stresses during transport in porous media [102–104]. As a result of such instabilities, chaotic flow fields can be generated, which are reminiscent of the instabilities witnessed in inertial turbulence, often referred to as elastic turbulence. These instabilities are principally a result of inhomogeneous flow fields, which in turn depend on the rheology of the polymer solution and the geometry of flow fields.

Kawale et al. [54], using microfluidics, found that flowing an HPAM solution in the presence of salt through porous media leads to two elastic instabilities. The first elastic instability exists during an apparent shear-thinning regime at $Wi \sim 80$ (see the left-hand side picture in Figure 1d) where stationary dead zones were formed around the obstacles. By increasing the flow rate to $Wi \sim 626$ (see the right-hand side picture in Figure 1d), the second elastic instability was observed where the dead zones became unstable. This was accompanied by strong temporal fluctuations in both pressure drop and flow field. The authors attributed the onset of shear-thickening to the second type of elastic instability.

Browne and Datta [105], using direct flow visualization in a 3D porous medium, showed that shear thickening is due to the onset of elastic instability in which the flow exhibits strong spatiotemporal fluctuations. They argued that the viscous dissipation caused by flow fluctuations leads to the anomalous increase in the apparent viscosity (η_{app}). They also quantitatively linked these flow fluctuations and the increase in the apparent viscosity using the following equation:

$$\frac{\eta_{app}(\mathrm{Q/A})}{\mathrm{k}} \approx \frac{\eta(\dot{\gamma}_I)(\mathrm{Q/A})}{\mathrm{k}} + \frac{\langle \chi \rangle_{t,\,V}}{(\mathrm{Q/A})} \tag{2}$$

The first term on the right-hand side denotes Darcy's law for a laminar steady flow ($\dot{\gamma}_I$ is the interstitial shear rate, Q is the flow rate, and A is the cross-sectional area). The second term denotes the additional contribution to the macroscopic pressure drop from viscous dissipation by the solvent, induced due to unstable flow fluctuations. $\langle \chi \rangle_{t,\,V}$ is the average rate of added dissipation as a result of flow fluctuations, which is measured using flow visualization over all the imaged pores. As expected, the overall rate of added dissipation increases as more pores become unstable, which leads to an increase in the apparent viscosity of the polymer solution.

3.2. Rheological Models for Polymer Flow through Porous Media

Most of the studies that have looked at modeling polymer rheology in porous media [31,106–110] have been based on the analytical and numerical solutions of non-Newtonian fluids. Comprehensive reviews on this subject have been given by Savins [111] and Sochi [112]. According to Sochi [112], there is no general methodology yet that can deal

with all cases of non-Newtonian flow in porous media. In the absence of a general approach, the continuum approach, capillary bundle models, and pore-scale network modeling have received greater attention. These approaches are briefly described below.

Continuum approach: In this model, the porous media is considered a continuum and its microscopic properties are translated into Darcy-scale parameters such as permeability. The Darcy and Blake–Kozeny–Carman equations are examples of continuum models. For a non-Newtonian flow such as a polymer solution, Darcy's law can be used to determine the polymer apparent viscosity (η_{app}) according to Equation (3):

$$\eta_{app} = \frac{k}{V_s}\frac{\Delta P}{L} \tag{3}$$

where k is the permeability, ΔP is the pressure drop across a porous medium with length L, and V_s is the superficial velocity in the porous medium. It should be noted that Darcy's law is valid only at a low Reynolds number where the flow is laminar. In addition, it considers only the viscous term and ignores the inertial term. However, at high superficial velocities, inertial effects are no longer negligible. Modifications to Darcy's equation are available to include these non-linearities using the homogenization or volume averaging method [113,114].

A semi-empirical Blake–Kozeny–Carman model is a microscopic approach that is used in fluid dynamics to determine the pressure drop from the superficial velocity of a fluid flowing through a granular packed bed of solids. According to this model, the polymer apparent viscosity can be calculated according to Equation (4):

$$\eta_{app} = \frac{\phi^3}{(1-\phi)}\frac{L}{\Delta P}\frac{\psi^2 D^2}{150}\frac{1}{V_s} \tag{4}$$

where ϕ is the bed porosity, ψ is the sphericity of the particles in the packed bed, and D is the diameter of the spherical particle [115].

Capillary bundle models: In this approach, it is assumed that the porous medium consists of parallel capillaries. For the simplest case where the capillaries are uniform and all have the same radius and length, the permeability is given by [116]:

$$k = \frac{\phi R^2}{8} \tag{5}$$

where R is the radius of each tube and ϕ is the porosity of the medium. This is a very simple approach to the porous medium. However, it works very well for the flow of (quasi-) Newtonian fluids. Nonetheless, this simplicity ignores several characteristics of the porous medium such as heterogeneity, converging–diverging nature, and morphology of pore space (e.g., pore size distribution and the tortuous character of any flow path). These ignored characteristics can be very important in modeling the flow behavior of the polymer solution in porous media. For instance, the tortuous character of the flow path causes the polymer molecules to be accelerated and decelerated and the converging–diverging nature of pore space strongly affects the flow of viscoelastic polymer solutions [112]. Capillary bundle models have been modified by considering a bundle of capillaries of varying cross-sections [117] to account for the tortuosity [118] and pore size distribution of porous media [119].

Pore-scale network modeling: The focus of the above two approaches is on providing an analytical solution for non-Newtonian fluid flow through porous media. However, the microscopic features of porous media are overlooked, as mentioned above. The modeling of viscoelastic behavior on the pore scale aims to take into account both macroscopic and microscopic features. Typically, in pore-scale network modeling, the porous media is considered as a connected network of capillaries [5]. To depict the flow through the network, a simplified form of flow equations is used. Then, to solve a system with multiple flow equations, in order to determine the flow field, a numerical approach is typically exploited.

Applying this methodology to a particular random network gives the macroscopic properties (e.g., the apparent viscosity) as a function of flow rate. Generally, the rheology of the polymer solution in the bulk phase and a pore space depiction of the porous media are used as inputs to the model. The pore-scale simulation begins with solving the flow equation for one single capillary as described in Equation (6):

$$Q = H\Delta P \tag{6}$$

where Q is the volumetric flow rate, ΔP is the pressure drop along the capillary, and H is the flow conductance that is dependent on the viscosity and pressure drop. To find the apparent viscosity of the polymer solution, a set of flow equations is solved for a connected network of capillaries with the assumption that mass conservation is satisfied. The inlet and outlet pressures of the network are set as boundary conditions. In Equation (6), the viscosity is pressure-dependent and unknown. Therefore, to begin, an initial guess for the viscosity is considered. Thereafter, the pressure field is solved iteratively and the viscosity is updated after each iteration cycle, up to the point where the convergence is achieved [120].

Pore-scale modeling of non-Newtonian fluid displacement in porous media based on a multiphase Lattice Boltzmann (LB) framework has also received attention in the literature [121–123]. According to Xie et al. [123], to account for the viscoelastic effects, the momentum equation is corrected by Maxwell's constitutive relation. This leads to the modification of the LB evolution equation for Maxwell fluids by removing the normal, but excess, viscous term. Their simulation results indicated that increasing either the intrinsic viscosity of the polymer solution or the elastic modulus leads to an improvement in oil recovery. Based on an LB model, Xie et al. [121] reported important mechanisms for the increase in the apparent viscosity of a viscoelastic fluid at high shear rates. These mechanisms consist of a decrease in the conductivity due to stagnant fluid, the compressed effective flow region, and more pronounced energy dissipations because of the viscoelastic instability.

Even though pore-scale network modeling is capable of envisaging the general trend of polymer flow through porous media, it still cannot comprise all the complexities. The limitations of this approach include the difficulty in identifying the deformation history of the polymer in the pore throats, the compromise in the viscoelasticity of the polymer solution due to the idealization of the void space, and the adoption of the no-slip-at-wall condition [112].

4. Polymer Retention in Porous Media

Polymer retention results from the interaction between polymer molecules in the solution and the porous media itself. It leads to the loss of polymer and, if this loss is significant, to a reduction in the viscosity of the polymer solution which in turn results in a decline in oil recovery. Therefore, polymer retention can have an enormous impact on the technical feasibility and economic viability of commercial polymer flooding projects.

4.1. Polymer Retention Mechanisms

There are three mechanisms for the retention of polymer in porous media: mechanical entrapment, hydrodynamic retention, and adsorption (see Figure 1b). Retention by mechanical entrapment occurs in porous media when larger polymer molecules become lodged in narrow pore throats [124]. This happens when polymer molecules are smaller than the inlet of the pore throats but larger than their outlet [125,126]. When polymer molecules become trapped in narrow pores, the pore size decreases, which increases the probability of trapping the smaller polymer molecules. This self-amplifying process ultimately leads to pore clogging.

Hydrodynamic retention is caused by an increase in the hydrodynamic forces acting upon the polymer molecules. Once equilibrium in polymer retention is reached, a sudden increase in flow rate will result in extra polymer loss in the porous media as some of the polymer molecules are trapped in stagnant flow regions by hydrodynamic drag forces. When the flow rate is reduced or flow is completely stopped, polymer molecules may

diffuse back to the main flow channels and the newly retained polymer molecules will be released; therefore, this phenomenon is reversible [124,127,128].

Adsorption takes place when there is an attractive interaction between the polymer molecules and the rock surface. Polymer adsorption onto the rock is considered a physical phenomenon and is a result of the high affinity of the polymer due to van der Waals forces and hydrogen bonding [129–131]. The polymer chain that is adsorbed forms a sequence of trains, loops, and tails. The trains are the polar groups along the polymer chain that are attached to the various polar points on the rock surface. The loops are those segments of the chain that are present between two trains and that stretch out into the solution. The tails exist at the ends of the polymer chain and have merely one end attached to the rock surface [56,132]. Even though some of the trains of the polymer chain might detach from the surface of the rock, other trains will remain in place. Once other trains detach, the formerly detached trains may reattach to the surface of the rock. Therefore, it is statistically very unlikely that a polymer chain would release all the attachment points simultaneously. This was explained by Zitha et al. [133] using a mechanism comprised of the following stages: (a) chain stretching in the zones where the flow is strongly extensional, (b) a transport short enough for the stretched chains not to be relaxed, and (c) adsorption by the formation of bridges across the smallest pore restrictions. If the ends of the molecules attach to the rock, a plugging or increased resistance to flow can develop.

Among the above three mechanisms, hydrodynamic retention is probably the one that contributes the least and is often neglected [6]. The relative importance of mechanical entrapment and adsorption depends on the ratio between the hydrodynamic radius of the polymer coil (R_h) and the pore radius (R_p). For $R_p > 50R_h$, which is almost always the case for high-permeability sands [128], polymer adsorption is the dominant mechanism, while for $R_p < 3R_h$, which is typical of low-permeability rocks, mechanical entrapment is dominant [124,126,128]. However, there are exceptions to this criterion. For instance, only 35.2% of the retention of an HPAM solution in a high-permeability silica pack (5.6 Darcy) was accounted for by adsorption and the remaining retention was attributed to mechanical entrapment and hydrodynamic retention. This discrepancy can be accounted for by the high heterogeneity of the tested silica pack [134].

4.2. Polymer Depletion and Inaccessible Pore Volume

If the size of the polymer chain is not negligible compared with the pore size, which is the case for low permeability rocks, the following consequences for polymer rheology may be expected: (a) in a non-adsorbent porous media, pore wall depletion excludes the polymer macromolecules from the slowest streamlines near the wall, thus giving a polymer velocity higher than the solvent velocity; (b) in an adsorbent porous media, the flow is modified due to adsorbed layer thickness [34].

The inaccessible pore volume (IPV) [124,135] accounts for the volume of the pores through which the large polymer molecules cannot flow. Several models and mechanisms have been proposed in the literature to explain the occurrence of IPV, including the relative size of pore throats, pore wall exclusion, and entropic effects [136–140]. As a result of the existence of IPV, polymer adsorption is reduced as there will be less contact between the polymer molecules and the rock surface.

4.3. Measurement of Polymer Retention in Porous Media

The measurement of polymer retention in the laboratory can be done in bulk or core-flood experiments. Bulk tests are usually referred to as static adsorption tests, which measure the change in polymer concentration when it is mixed with a crushed rock sample. Polymer retention in core-flood experiments is referred to as dynamic adsorption (DA). A polymer solution, together with a non-adsorbing tracer (commonly potassium iodide), is injected into the cores and the effluent is collected over time. Thereafter, the effluent is analyzed to determine the variation in the tracer and polymer with time and, thus, to find the level of adsorption (i.e., the comparison of the effluent concentration to the initial

polymer concentration). The two most frequently used methods in the literature to measure dynamic adsorption are described below.

In the first method, which is known as the single injection method, the polymer and tracer are co-injected and their normalized concentrations (i.e., the effluent concentration divided by the initial concentration) are plotted as a function of pore volumes (PV) injected. The DA is then determined by calculating the area between the polymer and the tracer curves and subtracting the IPV [135]. Alternatively, the DA can be calculated by reading the pore volumes of the injected tracer and the polymer where their normalized concentration is 0.5 and subtracting the IPV [124]. The disadvantage of the single injection method is that the IPV must be known in order to obtain an accurate result.

The second method, known as the double injection or extended injectivity method, is proposed by several authors [141–143]. In this method, two injection steps are taken. An illustration of these two injection steps is shown in Figure 3. In the first step, the polymer and tracer are co-injected. In this step, the tracer leads the polymer because of the polymer adsorption that delays the polymer advancement through the porous medium. The assumption here is that the injection of many pore volumes of the polymer solution leads to saturation of all the adsorption sites on the rock surface by the polymer molecules. In the second step, brine is first injected to displace all the mobile polymer and tracer, followed by the co-injection of polymer and tracer once again. In this step, adsorption no longer plays a role. Since some of the pores are not accessible to the polymer molecules but are to the tracer, the polymer leads the tracer. Consequently, the IPV is determined during the second step by calculating the difference between the areas of the tracer and the polymer curves according to Equation (7):

$$\mathrm{IPV} = \Sigma\left[\left(\left(\frac{C}{C_0}\right)_p - \left(\frac{C}{C_0}\right)_t\right) \times \Delta\mathrm{PV}\right] \tag{7}$$

where C and C_0 are the effluent and initial polymer concentration respectively, ΔPV is the pore volume increment for each effluent sample, and where subscripts p and t refer to polymer and tracer, respectively. It should be noted that this IPV, measured in the presence of adsorbed polymer, could be different from the IPV of the bare porous medium before any adsorption has taken place. The DA is then determined from the first injection step by using Equation (8):

$$\mathrm{DA} = \frac{\Sigma\left[\left(\left(\left(\frac{C}{C_0}\right)_p - \left(\frac{C}{C_0}\right)_t\right) \times \Delta\mathrm{PV}\right) + \mathrm{IPV}\right] \times (C_0)_p \times \mathrm{PV}}{m} \tag{8}$$

where m is the rock mass.

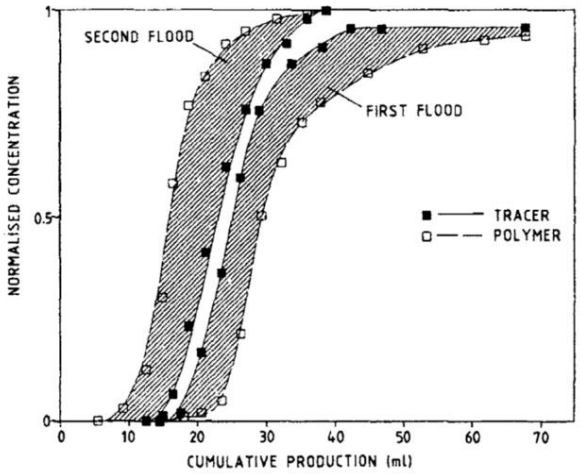

Figure 3. The tracer and polymer normalized concentration profiles in the effluent in the double-injection method for polymer retention measurement in porous media. Adapted with permission from [142].

4.4. Modeling of Polymer Retention

To model the polymer retention in porous media, simulators such as UTCHEM and Eclipse consider a Langmuir type isotherm. In this approach, polymer retention is modeled as a function of polymer concentration, salinity, and permeability according to Equation (9) [144]:

$$\widehat{C_4} = \min\left[\widetilde{C_4}, \frac{a_4\left(\widetilde{C_4} - \widehat{C_4}\right)}{1 + b_4\left(\widetilde{C_4} - \widehat{C_4}\right)}\right] \tag{9}$$

where $\widehat{C_4}$ and $\widetilde{C_4}$ are the polymer retention and concentration, respectively. The minimum is taken to ensure that the polymer retention is smaller than the total polymer concentration. a_4 is defined as:

$$a_4 = (a_{41} + a_{42}C_{SEP})\left(\frac{k_{ref}}{k}\right)^{0.5} \tag{10}$$

C_{SEP} is the effective salinity that is described as follows:

$$C_{SEP} = \frac{C_{51} + (\beta_p - 1)C_{61}}{C_{11}} \tag{11}$$

where C_{51}, C_{61}, and C_{11} are the anion, divalent cation, and water concentrations in the aqueous phase and β_p is the covalent coefficient that is known from laboratory experiments. The value of a_4/b_4 characterizes the highest amount of adsorbed polymer and b_4 controls the curvature of the isotherm. The reference permeability (k_{ref}) is the permeability at which the input adsorption parameters are stated.

5. Factors Influencing Polymer Performance in Porous Media

5.1. Polymer Type

As discussed, high molecular weight synthetic polymers such as HPAM exhibit shear-thickening behavior in porous media due to their flexible coil conformation. However, such shear-thickening behavior is absent for biopolymers such as xanthan gum and scleroglucan due to their rigid rod-like conformation. They are likely to align in the flow field and to remain shear-thinning instead of showing viscoelastic behavior [145–147]. Biopolymers have also shown significantly lower retention in porous media compared with synthetic polymers [52,56]. For synthetic polyacrylamides, the degree of hydrolysis plays an important role in polymer retention and, as it increases, the polymer retention in porous media decreases [148]. Lecourtier et al. [149] observed that the retention of a non-ionic polyacrylamide (PAM) solution with pH 7 onto a SiC surface was dramatically higher than that of HPAM with a degree of hydrolysis of 30%. This was because the negatively charged surface of SiC at pH 7 gives rise to a repulsion term once it interacts with the negative charges present in the HPAM chain. The retention of PAM and HMPM were comparable only at a salinity of 2.4 wt% (24,000 ppm), where the negative charges along the HPAM are screened.

Modifying the polymers (as will be discussed in Section 6) can also influence polymer adsorption and retention. Szabo [150] showed that the adsorption of poly(2-acrylamido-2-methyl-1-propanesulfonic acid) commonly known as AMPS, is lower than HPAM. Vermolen et al. [151] also reported that the incorporation of AMPS, as well as N-vinyl pyrrolidone (N-VP) into HPAM, can dramatically reduce its retention.

5.2. Polymer Molecular Weight

Higher molecular weight, i.e., longer polymer chains, implies higher viscosifying power and potentially higher resistance to flow in porous media. However, flow resistance, also referred to as injectivity decline, can be a time-dependent phenomenon [125,152], as higher molecular weight polymers are more sensitive to mechanical degradation. Mechanical degradation will be more likely to occur in extensional flow fields, but some degradation

of polymer chains with very high molecular weight (or degree of polymerization) may also occur in pure shear flows [153]. Odell et al. [154] predicted that in the dilute regime, when there is a continuous increase of stress on the middle of the polymer chain, mid-chain scission will occur, beyond a critical strain rate referred to as the critical fracture ($\dot{\varepsilon}_f$). As the relaxation time increases with the length of the polymer chain, Wi is larger for the longest chains compared with the shortest chains. Therefore, the higher molecular weight polymers are more likely to experience the mid-chain scission than the lower molecular weight ones. Several experimental papers have shown that mid-chain scission is induced by a transient extensional flow field [155,156] as well as an ultrasonic cavitation [157,158].

The effect of molecular weight on polymer retention has also received attention. Dang et al. [159] reported a simulation study showing that the maximum adsorption of HPAM was obtained with the lowest molecular weight in good agreement with an experimental study [160], in which adsorption of HPAM on Berea sandstone decreased with increasing molecular weight. In some studies, however, with increasing molecular weight, the adsorption level first increased and then became constant [161,162].

5.3. Polymer Concentration Regimes

Depending on the target viscosity, polymer solutions may be used at different concentrations. Several authors have proposed that HPAM retention is dependent on the polymer concentration regime [126,135,163,164]. In the semi-dilute regime, polymer retention increases with increasing concentration, and Szabo and Corp [126] suggested that the concentration dependence of HPAM adsorption in the semi-dilute regime is linear. In the dilute and concentrated regimes, on the other hand, polymer retention is basically concentration-independent [163]. This implies that a Langmuir isotherm can describe the concentration dependency of the polymer retention [165] (see Section 4.4). Furthermore, polymer chain scission is also concentration-dependent. In the dilute regime, beyond the critical fracture, the mid-chain scission occurs and the polymer chain is broken almost precisely in half, whereas in the semi-dilute regime, with increasing the polymer concentration, the chain scission does not occur in the center of the chain and is increasingly randomized [166].

5.4. Porous Media Permeability

When the retained polymer molecules form an adsorption layer on the rock surface, the effective pore size is reduced, resulting in a decrease in the rock permeability or an increase in the residual resistance factor. This phenomenon typically becomes more severe when the rock permeability is smaller than 500 mD [167–170]. In such lower-permeable rocks (<500 mD), the polymer retention also increases dramatically with decreasing permeability. Vela et al. [168] measured the polymer retention from the material balance of injected and produced fluids and found that the retention of HPAM increases from ~12 μg/g in 137 mD sandstone to ~130 μg/g in 12 mD sandstone. In contrast, in higher permeability rocks, polymer retention is generally insensitive to permeability [65].

5.5. Residual Oil Saturation

In water-wet cores, the presence of residual oil in the core has little effect on the polymer retention [171], or even reduces it [126,142,172], compared with oil-free 100% brine-saturated cores. However, in contradiction to these findings, Hughes et al. [142] observed that the retention of xanthan gum in 127 mD Berea sandstone increased in the presence of residual oil. The authors ascribed this phenomenon to the increase in polymer trapping caused by the reduction, due to the presence of the oil, of the core permeability. The effect of residual oil on polymer retention may be different in oil-wet cores. Broseta et al. [171] described that the existence of residual oil (iso-octane) saturation in oil-wet cores significantly decreased the HPAM retention by a factor of 2–5.

5.6. Iron and Clay Content

The presence of iron and clay can strongly affect the surface properties of the core [173]. The point of zero charge (PZC) for pure quartz is reported to be 1–3 [149,174,175]. Farooq et al. [176] reported that the PZCs of Bentheimer and Berea sandstone samples were approximately 3.0 and 8.2, respectively. In their experiments, the quartz fractions for Bentheimer and Berea sandstone samples were found to be approximately 98.0% and 82.5%, respectively, whereas the clay fractions were approximately 0.5% and 9.0%, respectively. Peksa et al. [177], whose Bentheimer sample had a quartz fraction of approximately 92%, measured a PZC of nearly 8. This unexpectedly high PZC was attributed to the presence of clay (~2.7%) and iron particles (~0.2%) distributed within the sample.

Clay particles are well distributed in sandstone and become mobile in contact with fluids at a pH higher than 8 [178,179]. The higher the pH, the more visible the effect is. In addition, the effect of the iron minerals, such as goethite and hematite, present in sandstone on the PZC was observed. Iron oxides represent a PZC in the range of 8.5–11 [180]. This suggests that even a small proportion of iron and clay content, if well distributed in the rock, can dramatically increase the PZC of the sandstones. Further work on the effect of iron and clay particles on the PZC of sandstone is needed. A PZC of 8 for sandstone leads to a positively charged rock surface at an injected water pH of around 7, which results in increased interactions with negatively charged polymers such as HPAM or xanthan gum.

5.7. Salinity and Hardness

Salinity and hardness have been associated with two major effects on polymer performance in the literature: viscosity loss and polymer precipitation. For synthetic polymers, namely HPAM, the viscosity loss at high salinities has been ascribed to the shielding of the electric charges along the polymer chain [181]. Since high molecular weight HPAM has a flexible coil conformation, it responds strongly to the ionic strength of the aqueous solvent [52]. At high salinities, the negative charges along the HPAM backbone are screened, leading to a reduction in electrostatic repulsion and a shrinking of the polymer coils in the solvent. The end result of this process is a relatively lower hydrodynamic radius of the polymer coils. The reduction of the hydrodynamic radius of the polymer coils results in viscosity loss.

In addition, a major challenge for the use of HPAM at high salinities is the presence of a high concentration of divalent cations such as Ca^{2+} and Mg^{2+}. In the presence of the divalent cations, polyion–metal complexes can be formed, which in turn leads to polymer precipitation due to the complexing ability of the carboxylate groups of HPAM [182,183].

Biopolymers, such as xanthan gum, have shown less sensitivity to salinity and hardness compared with synthetic polymers. At high salinities, the structure of the xanthan gum backbone experiences a conformational alteration from a disordered conformation to an ordered and more rigid structure (coil–helix transition) [184–186]. As a result of the rigidity of the polymer chain, xanthan gum is less sensitive to the presence of ions in the solvent compared with HPAM.

5.8. Temperature

High salinity and hardness in oil reservoirs are often accompanied by high temperatures. Viscosity loss and polymer precipitation of HPAM become more severe at elevated temperatures, as the further hydrolysis of the polymer backbone is promoted. This causes additional interaction between the charged polymer backbone and the ions in the solvent. Moradi-Araghi and Doe [187] suggested a temperature stability limit for HPAM based on the cloud point and the rate of hydrolysis. They demonstrated a "safe" limit of approximately 75, 88, 96, and 204 °C for HPAM in brines containing 2000, 500, 270, and 20 ppm hardness, respectively. They suggest that even a small concentration of divalent cations at high temperatures can substantially hinder the use of HPAM.

A helix–coil transition occurs in the structure of xanthan gum at high temperatures, which causes a reduction in the viscosity. However, compared with HPAM, xanthan gum

is more resistant to high temperatures due to its more rigid backbone. Long-term stability experiments carried out using a commercial xanthan gum showed that the solution viscosity remained almost unchanged for about 2 years at 80 °C [188].

A common way of assessing the long-term stability (ageing) of polymers at combined high salinity, hardness, and temperature is to keep the samples in an oven for up to one year and monitor the viscosity loss or polymer precipitation over time. Alternatively, thermal gravimetric analysis (TGA) can be used to assess the polymer resistance to thermal degradation [189–191]. For long-term stability experiments, the polymer samples should be completely de-oxygenated (i.e., the experiments should be performed in anaerobic conditions). This is needed to ensure that viscosity loss is only due to the effect of high salinity, hardness, and temperature rather than the effect of a free radical attack caused by the presence of oxygen in the samples.

6. Advanced Water-Soluble Polymers

The synthesis of advanced water-soluble polymers, with higher temperature and/or salt tolerance, has been reported by several authors. These modified polymers are listed in Table 1. They were typically obtained by hydrophobically modifying conventional polymers or by the incorporation of salt- and temperature-tolerant monomers such as 2-acrylamido-2-methyl-1-propanesulfonic acid (AMPS) and n-vinyl pyrrolidone (N-VP) to the HPAM backbone.

In the literature, the experiments that investigate the effectiveness of modified polymers at high-salinity and high-temperature conditions fall into the following three categories: (a) the viscosity of the modified polymer is compared with the viscosity of a conventional polymer such as HPAM, both dissolved in brine [189,192], (b) the viscosity of the modified polymer dissolved in brine is compared with its viscosity in de-ionized (DI) water [147,193,194], and (c) the viscosity of the modified polymer is measured in brine with different compositions and ionic strengths [147,189,193,195]. Such experiments are often performed at various temperatures and consider both short- and long-term temperature effects on the performance of the modified polymers. In the following sections, a summary of these investigations is given and the mechanisms for the enhanced performance of polymers at high salinity and high temperature are discussed.

6.1. Hydrophobically Modified Polymers

Hydrophobically modified polyacrylamides (HMPAM), also known as associative polymers, differ from the conventional polyacrylamides used for cEOR, as they have small hydrophobic units in the polymer chain. Several hydrophobic monomers, for example, acrylate or alkyl groups with different topologies and number of carbons, have been used as the hydrophobic units of these polymers [196–198]. The fraction of hydrophobic units should be minimized to ensure the solubility of the polymer in water. However, even a small hydrophobic fraction can significantly change polymer properties.

Hydrophobically modified polyacrylamides are synthesized using different techniques such as micellar [199–201], homogeneous, and heterogeneous polymerization [199]. The hydrophobic units may be distributed in various ways through the polymer, such as randomly or block-like [40,197,199,202–205], and they can be coupled at one or both ends [206–211]. The distribution of the hydrophobic groups as a result of micellar copolymerization is block-like, while solution copolymerization results in a random distribution.

(a) General properties

Hydrophobic–hydrophobic interactions among the polymer chains result in either intra- or inter-molecular associations or their combination. An illustration of the concept of intra- or inter-molecular associations for a hydrophobically modified polyacrylamide is shown in Figure 4. The dominance of either association type depends on the polymer concentration and has a strong impact on the viscosity of the polymer solution. In the dilute regime, HMPAM forms more intra-molecular associations than intermolecular ones, twisting the macromolecular chains and reducing the hydrodynamic radius, thus

reducing the viscosity. At concentrations higher than the critical association concentration (CAC), inter-molecular associations become more dominant, which abruptly increases the hydrodynamic radius of the polyacrylamides [212–216].

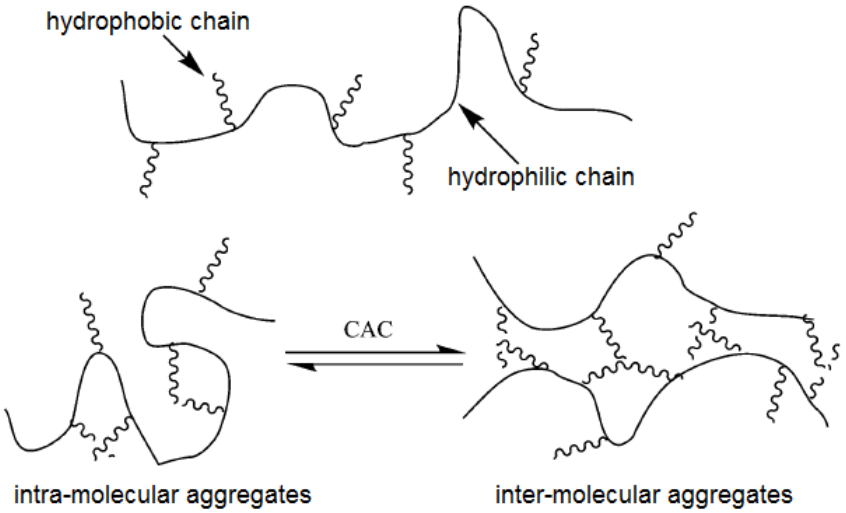

Figure 4. Intra- and inter-molecular associations in a hydrophobically modified polyacrylamide. Adapted with permission from [216].

(b) Effect of salinity

Several authors have reported that the addition of salt can enhance the viscosity of hydrophobically modified polyacrylamides [197,217,218]. The reason for this appears to be that, by screening the electric charges along the chains with the salts, the electrostatic interactions are suppressed. As a result, the hydrophobic associations are less likely to be disrupted by electrostatic interactions and this results in a higher solution polarity. The higher polarity leads, in turn, to the reinforcement of the hydrophobic associations, which allows the formation of aggregates and a stronger network through inter-molecular hydrophobic associations [219]. Therefore, an increase in the viscosity of the solution is expected in the presence of salt (see polymers 1, 2, 3, and 4 in Table 1).

However, upon a further increase in salinity, the hydrophobic aggregates become more compact. These condensed aggregates then associate to form larger aggregates, which results in the phase separation of the polymer and a reduction in the viscosity [197,220]. For instance, Al Sabagh et al. [221] reported a rheological study of three HMPAMs [222] at 30 °C. The authors found that, first, the viscosity increases with increasing NaCl concentration up to 2.9 wt% (salt thickening) and, then, above this value, the viscosity decreases as the NaCl concentration increases (salt thinning) (see Figure 5a). Rather similar behavior was observed for $CaCl_2$ concentration. However, the transition from salt-thickening to salt-thinning behavior occurs at a much lower concentration for $CaCl_2$ (0.2 wt%) (see Figure 5b). Zhong et al. [223] suggested that salt-thickening behavior can occur at two ranges of salinities (2–3 wt% and 5–9 wt%) but, at salinities higher than 9 wt%, the viscosity decreased.

More recently, Mirzaie Yegane et al. [224] showed that HMPAM in a brine containing 20 wt% NaCl and 1.5 wt% Ca^{2+} has a viscosity some 55% higher than its viscosity in DI water, regardless of HMPAM concentration. This exceptional viscosity increase at high salinity was attributed to the excellent solubility of the HMPAM in both brine and DI water, as well as the increase in solvent viscosity, which was measured to be 0.9 ± 0.1 and 1.4 ± 0.1 mPa s for DI water and brine, respectively. It is our understanding that the solubility of the hydrophobic group plays a key role in maintaining the viscosity with increasing salinity and hardness. Therefore, it is recommended to estimate the solubility limit of the hydrophobic comonomers prior to polymerization to decide on (a) the type of hydrophobic group and (b) the fraction of hydrophobic units to be incorporated into the polymer backbone.

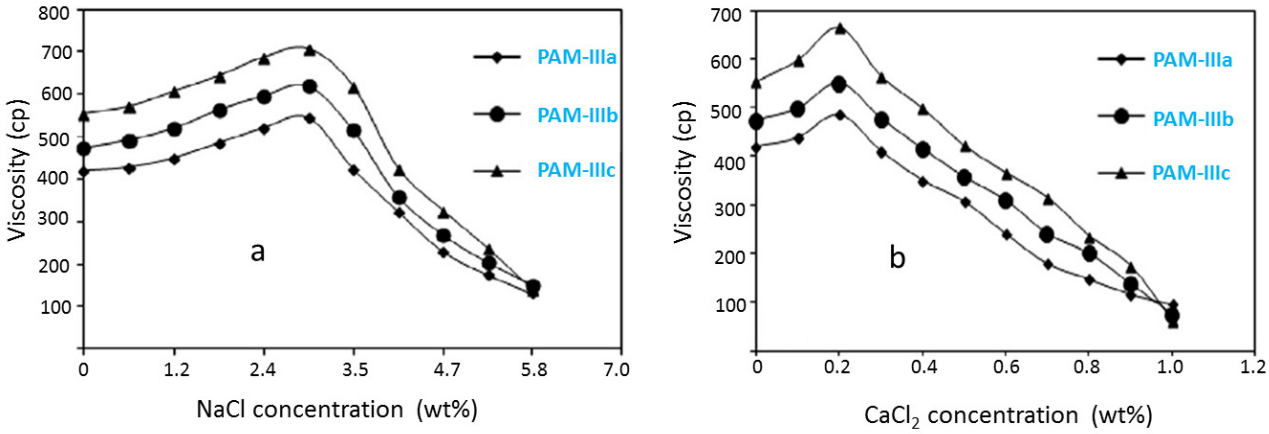

Figure 5. Effects of (**a**) NaCl and (**b**) $CaCl_2$ concentration on the viscosity of hydrophobically modified polyacrylamides at 30 °C. Adapted with permission from [221].

(c) Effect of temperature

For both compositional and structural reasons, the behavior of the HMPAMs is significantly affected by temperature. An increase in temperature improves the solvent quality of the hydrophilic segments of the HMPAM. This will tend to increase the hydrodynamic radius of the chains. At the same time, the solvent quality for the hydrophobic segments will deteriorate. Therefore, the hydrophobic units will have an increased tendency to form stable networks. Both effects could lead to an increase in viscosity as temperature increases.

The increase in the viscosity of the HMPAMs with increasing temperature is also explained by the concept of so-called thermo-thickening copolymers (also known as thermo-associative and thermo-stimulated copolymers) [225–227]. This concept is based on the switch properties of polymers characterized by a lower critical solution temperature (LCST). These polymers have a highly water-soluble macromolecular backbone, with some LCST side chains or blocks (see Figure 6). With increasing temperature, these thermo-sensitive moieties can undergo reversible micro-phase segregation. Above the CAC, this change results in an increase in the solution viscosity through inter-molecular associations. It is noteworthy that the thermo-thickening behavior of the polymer solution is more evident at low salinities and shear rates [228].

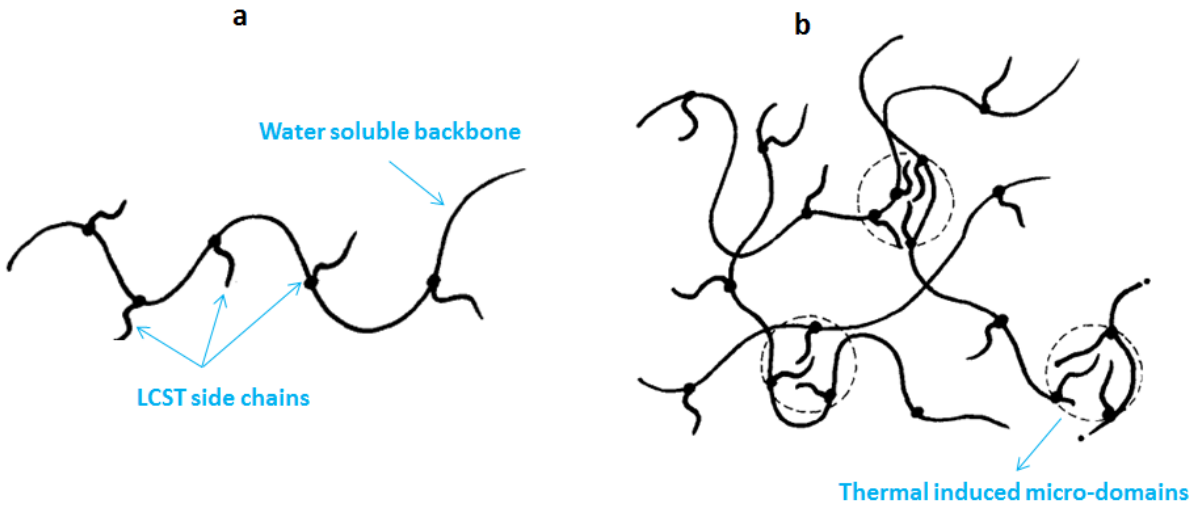

Figure 6. Thermo-associative concept in aqueous solutions: (**a**) copolymer structure; (**b**) association mechanism (T > LCST). Adapted with permission from [227].

The viscosities of solutions of polymer numbers 5 or 6 in Table 1 are not significantly dependent on the temperature when in the range of 30–60 °C [229,230]. The intrinsic viscosity of a solution containing polymer number 7, rose from 6.5 to 8.5 dL/g as the temperature increased from 25 to 60 °C [231]. Thermo-thickening behavior at low ionic strength and shear rate was observed with polymer number 8 [232]. This was ascribed to the increase in the concentration of poly(propylene oxide) (PPO) in the hydrophobic micro-domains. This resulted in an increase in chain mobility at fairly high temperatures. With a further increase in the temperature, the viscosity of the hydrophobically modified polymers is expected to decrease. This is ascribed to the loss in the network connectivity because of changes in the hydrophobic micro-domains.

Even though hydrophobically modified polymers can enhance the solution viscosity at moderately high salinity and temperature, their application at higher salinity (>5 wt% TDS) and higher temperature (>80 °C) is challenging. This becomes more difficult, in particular when high salinity and high temperature coexist in a reservoir where the polymer solution viscosity will potentially be strongly reduced.

6.2. Salt- and Temperature-Tolerant Modified Polyacrylamides

Several researchers have attempted to synthesize modified polyacrylamides with both salt- and temperature-tolerant comonomers, in order to enlarge the envelope of polymer flooding at high-salinity and high-temperature conditions. The synthesis attempts were based on the modification of polyacrylamide by the incorporation of one or more of the monomers that can enhance the stability of the polymer in such conditions (see polymer numbers 9 through 16 in Table 1). For instance, the incorporation of AMPS or acrylamido-tert-butyl-sulfonate (ATBS) to polyacrylamide increases the tolerance to high salinity and hardness [41,233,234]. The incorporation of N-VP to polyacrylamide, on the other hand, seems to protect the polyacrylamide units against hydrolysis.

Stahl et al. [235] studied a wide range of synthetic and biopolymers at an elevated temperature and moderately high salinity (121 °C and 3.3 wt% TDS). They found that the incorporation of N-VP in acrylamide prevents precipitation of the polymer at this temperature. They also observed that N-VP limits the level of acrylamide hydrolysis and argued that this gives the copolymer its enhanced stability in high salinity and hardness brines. Vermolen et al. [151] studied the effect of HPAM modification with AMPS and/or N-VP monomers, with the aim of maintaining the viscosity at an elevated temperature (120 °C) and high salinity (20 wt% TDS) in both the absence and presence of divalent ions (up to 1.8 wt%). They found that, in the absence of divalent ions (no hardness), HPAM is stable for more than 180 days. Unfortunately, the incorporation of 20–25 mol% AMPS to HPAM did not enhance the resistance against the presence of divalent ions at high temperatures. However, a terpolymer including acrylamide, 20–25 mol% AMPS, and 35–50 mol% N-VP monomers did stabilize the polymer in such harsh conditions.

Table 1. Polymers stable at high salinity and/or high temperature.

	Polymer	Salinity (ppm)	Temperature (°C)	Ref.
No.1	Hydrophobically modified polyacrylamide with methylene	100,000	25	[236]
No.2	Hydrophobically modified polyacrylic acid with alkyl acrylate	40,000	25	[237]
No.3	Hydrophobically modified polyacrylic acid with 2-(N-ethylperfluorooctanesulfoamido) ethyl acrylate (FA) or 2-(N-ethylperfluorooctanesulfoamido) ethyl methacrylate (FMA)	19,000	25	[219]
No.4	Hydrophobically modified polyacrylamide with *N*-phenethylacrylamide	90,000	25	[238]
No.5	Terpolymers of acrylamide (AM) with sodium 3-acrylamido-3-methylbutanoate (Na-AMB) and 2-acrylamido-2methylpropanedimethylammonium chloride (AMPDAC)	30,000	30–60	[229]

Table 1. *Cont.*

	Polymer	Salinity (ppm)	Temperature (°C)	Ref.
No.6	Hydrophobically modified polyacrylic acid with 3-pentadecylcyclohexylamine (3-PDCA)	0	30–60	[230]
No.7	Hydrophobically modified polyacrylamide 3-(2-acrylamido-2-methylpropanedimethylammonio)-l-propanesulfonate (AMPDAPS)	0	25–60	[231]
No.8	Poly(propylene oxide) methacrylate	0	25–70	[232]
No.9	Thermoviscosifying polymers (TVP) mainly based on thermosensitive poly(*N*-isopropylacrylamide) (PNIPAM) and polyethylene (PEO)	33,000 (TDS), 900 (DC)	90	[239]
No.10	Copolymer of hydrolyzed polyacrylamide (HPAM) and 2-acrylamido-2-methylpropane sulfonic acid (AMPS)	50,000	80	[233]
No.11	Incorporation of Acrylamido-Tert-Butyl-Sulfonate (ATBS) and/or N-vinyl pyrrolidone (N-VP) into hydrolyzed polyacrylamide (HPAM)	500–100,000	85–140	[234]
No.12	Synergy of hydrolyzed polyacrylamide (HPAM) and 2-acrylamido-2-methylpropane sulfonic acid (AMPS) with surfactant	172,000	95	[240]
No.13	Incorporation of sodium 2-acrylamido-2-methylpropane sulfonic acid (Na-AMPS) and/or N-vinyl pyrrolidone (N-VP) and/or sodium 3-acrylamid 3-methyl butyrate (N-AMB) and/or N-vinyl amide (N-VAM) into hydrolyzed polyacrylamide (HPAM)	34,600–180,000 (TDS)	90–120	[241]
No.14	Incorporation of Acrylamido-Tert-Butyl-Sulfonate (ATBS) and/or N-vinyl pyrrolidone (N-VP) into hydrolyzed polyacrylamide (HPAM)	13,000 (TDS), 7000 (DC)	85	[242]
No.15	Copolymer of 2-acrylamido-2-methylpropane sulfonic acid (AMPS) and hydrolyzed polyacrylamide (HPAM)	170,000 (TDS), 17,000 (DC)	100	[41]
No.16	Incorporation of sodium 2-acrylamido-2-methylpropane sulfonic acid (Na-AMPS) and/or N-vinyl pyrrolidone (N-VP) into hydrolyzed polyacrylamide (HPAM)	43,700–179,800 (TDS), 2100–17,700 (DC)	120	[151]

6.3. Polymer–Nanoparticles Hybrid

An alternative approach is to use a hybrid of polymer and silica nanoparticles (NPs) to create a hybrid system with enhanced rheological properties under harsh conditions [243]. This novel approach is based on the idea that the rheological properties of the hybrid can be fine-tuned by controlling the interactions between the polymer and the silica NPs. Silica NPs have been the most frequently used NPs for cEOR due to their potential to change the rock wettability and to reduce the IFT [244]. The surface properties of silica NPs can be changed from hydrophobic to hydrophilic by silanization with hydrophilic hydroxyl groups, hydrophobic sulphonic acid, or hydrophilic polyethylene glycol [245]. Moreover, silica NPs have shown a good thermal stability [246].

Silica NPs can also adjust the properties of the base fluid, for instance, the fluid density, viscosity, and heat tolerance [247,248]. In particular, the addition of silica NPs to a polymer solution can improve its viscosity and enhance its heat tolerance [249–251]. The interaction between polymer molecules and silica NPs has mainly been attributed to hydrogen bonds between the functional groups on polymer molecules including hydroxyl, amide, and carboxylate groups and the silanol groups on the surface of silica NPs [250,252–254]. Hence, silica NPs can act as physical crosslinkers between polymer chains, which reinforces the molecular network structure. As a result, a structure with a larger hydrodynamic volume will be formed and the movement of polymer chains becomes limited, which in turn results in an increase in the polymer solution viscosity [224,254].

Some researchers have discussed that the hybrid networks based on reversible associations can be obtained by the inclusion of silica NPs into the macromolecular architecture

of associative polymers [55,255–258]. Temperature and salting out can be employed to adjust the viscoelastic properties of a hybrid network of polymers and NPs [255]. For instance, Portehault et al. [55] reported that the addition of silica nanoparticles into a polyacrylamide having poly-(*N*-isopropylacrylamide) (PNIPA) as LCST side chains results in specific interactions between the polymer side chains and the silanol groups on the surface of nanoparticles, leading to a physical hybrid network in the whole temperature range. Upon heating, unbound PNIPA grafts self-assemble into nanodomains and improve the viscoelastic properties and connectivity of the hybrid (see Figure 1e).

Bhardwaj et al. [253] observed enhanced thermal stability for nano-size polyacrylamide–silica composites. Maghzi et al. [259] showed the viscosity of a hybrid of polyacrylamide–silica was larger than the viscosity of the polyacrylamide solution for salinities ranging from 1.4 wt% to 8.4 wt% TDS. Hu et al. [252] noted the introduction of silica NPs significantly enhanced the HPAM viscosity at salinities up to 8 wt% NaCl and temperatures up to 80 °C. Cao et al. [254] reported that the resistance of a copolymer of acrylamide and AMPS against high-salinity and high-temperature conditions was enhanced upon the addition of amino-functionalized silica NPs at salinities up to 8 wt% NaCl and 0.12 wt% $CaCl_2$ at 70 °C.

However, the above approaches suffer from some drawbacks: (a) no polymer–NP hybrid was studied for salinities higher than 8.4 wt%, (b) the colloidal stability of the hybrid system at high salinities appears to be challenging, and (c) the effect of the concentration of polymer on the rheological response of hybrids was not investigated.

To address these limitations, more recently it was proposed that enhanced stability and increased viscosity can be achieved at very high salinity (20 wt% TDS), hardness (1.5 wt% Ca^{2+}), and elevated temperature (70 °C) by the hybridization of hydrophobically modified polyacrylamide with hydrophobically modified silica NPs [224]. The surface of hydrophilic silica NPs was coated by gamma-glycidoxypropyltrimethoxysilane (GPTMS), a low-molecular-weight organic ligand where GPTMS covalently binds to the surface of NPs. This not only offers steric stabilization and establishes colloidal stability at high salinities, but it also shifts the surface of NPs from hydrophilic to hydrophobic. Hydrophobically modified nanoparticles facilitate the bridging between hydrophobically modified polyacrylamide chains. As a result, in the semi-dilute regime, where polymer chains were closer to one another, they could be bridged by NPs through hydrophobic–hydrophobic interactions. This enlarges the hydrodynamic volume of the hybrid and therefore increases its viscosity.

The results found in the literature demonstrate the potential of a polymer–NP hybrid as an alternate approach for enhanced oil recovery at high-salinity and high-temperature conditions. However, long-term thermal stability at high temperatures, which is a vital aspect of polymers in cEOR field applications, seems challenging. Even though organic ligands can provide the colloidal stability of NPs at high salinities, the situation at high temperatures in the long term can be different. The epoxy functional groups of an organic ligand can react/open up at high temperatures [260]. This leads to a reduction of the grafting density of the ligand and consequently a decrease in the steric potential. As a result, NPs can aggregate to each other, which (a) reduces the viscosity of hybrids and (b) makes their transport in porous media difficult and causes potential plugging and injectivity problems [245]. Therefore, further research on the development of organic ligands that are compatible with high-temperature conditions in the long term is essential.

7. Polymer Flooding in Practice

Several authors have proposed criteria for polymer flooding projects based on the effects of the parameters discussed in Section 5. There is a consensus about the fact that, prior to any field applications, laboratory experiments should be carried out to assess the feasibility of a polymer flooding project and to estimate the probability of success [261,262]. Specific criteria in laboratory experiments to enhance the chances of success of a polymer flooding project include the following: (a) meeting the target viscosity at reservoir conditions, (b) good filterability to ensure good injectivity, (c) suitable solubility

in brine, and (d) maintaining stability and viscosity under the influence of degrading factors such as shearing, heating, salinity, and hardness [261].

Table 2 shows the range of parameters for polymer flooding in laboratory experiments compared with real field applications. Table 3 gives a summary of these parameters in different field projects that have been performed recently.

Table 2. Range of parameters for polymer flooding in laboratory vs. field applications [22,261,262].

Parameter	Laboratory Experiments	Field Applications
Polymer type	HPAM Xanthan gum Associative polymer	HPAM Xanthan gum Associative polymer
Polymer molecular weight (g/mol)	1–25 × 10^6	12–25 × 10^6
Polymer concentration (ppm)	30–10,000	300–4000
Permeability (mD)	2.5–13,000	>50
Porosity (%)	10–47	4–37
Oil viscosity (cP)	1.7–5500	<5000
Lithology	Sandstone cores Carbonate cores Sand-packs Micromodels	Majority in sandstone reservoirs Very few in carbonate reservoirs
Water salinity (ppm)	250–186,000	Majority < 50,000
Temperature (°C)	20–120	<99

A summary of the range of parameters in the laboratory experiments, as shown in Table 2, is as follows. HPAM, xanthan gum, and associative polymers have been extensively used in laboratory experiments. There is a wide range in both the molecular weight (1–25 × 10^6 g/mol) and the concentration (from 30 up to 10,000 ppm) of these polymers in the performed experiments. The salinity of the water, in which the polymers are dissolved, is as high as 186,000 ppm. The experiments are performed at temperatures of up to 120 °C. Moreover, in laboratory experiments, the behavior of the polymers is studied in various types of model porous media, including sandstone and carbonate cores, sand-packs, and microfluidics. The permeabilities of these porous media range from very low (<10 mD) to very high (>13,000 mD) and the porosity ranged from 10 to 47%.

As can be seen in Table 3, in field applications, HPAM is the most commonly used polymer by far and the associative polymers were used only in a few projects (SZ36-1 and Bohai Bay in China, East Bodo and Mooney in Canada). As for the polymer molecular weight and concentration, the selected range for field applications is more limited than the laboratory experiments. The main motivation behind this is to avoid the injectivity problems, which can be a result of the high concentration and molecular weight of the injected polymer solution. The range of polymer molecular weights used is strongly dependent on reservoir permeability. High-molecular-weight polymers (>17 × 10^6 g/mol) have been used in reservoirs with an average to high permeability (>400 mD).

In contrast to the laboratory experiments, polymer injection has rarely been used in carbonate reservoirs in field applications and its use is mainly limited to sandstone reservoirs. The salinity of the injected water in the majority of field applications is lower than 50,000 ppm. It should be noted that for the Dalia/Camelia field in Angola, the formation water salinity was 117,000 ppm but the injected water salinity was 24,900 [263,264].

Song et al. [265] reviewed the most recent advances in polymer flooding projects in China. They reported that several salt-resistance polymers were developed for field projects in China, mostly for the Daqing field. These polymers include DS800, DS2500, and LH2500 with molecular weights of 8, 25, and 25 MDa, respectively. The chemical structure and synthesis of these polymers are explained in [266,267].

Successful field applications with very high salinity in the injected water are scarce. In the Bockstedt field in Germany (54 °C, injection water at 186,000 ppm) schizophyllan was used, but, despite good injectivity, considerable biological degradation was observed even in the presence of biocide [268,269]. In the Asab field in the UAE (120 °C, injection water at 270,000 ppm), the use of an ATBS-modified polyacrylamide (SAV 10) resulted in a successful injection in 2019 [270]. The lack of many successful projects in harsh conditions inspires the need for polymers that are stable at high salinity, especially in situations where there are high temperatures that can worsen the degradation effects. As discussed in Section 6, the recent advanced water-soluble polymers for high-salinity and high-temperature conditions can be good candidates for field projects in harsh conditions. However, more elaborative experimental studies, including ensuring good injectivity in lower permeability reservoirs and long-term stability tests that reflect the polymer lifetime in field projects, are needed to ensure their successful application on the field scale.

Table 3. Range of parameters in recent polymer flooding field applications (1 MDa = 10^6 g/mol, NR = not reported).

Country	Field	Formation Water Salinity (ppm)	Temperature (°C)	Oil Viscosity (cP)	Polymer Type	Polymer Concentration (ppm)	Polymer Viscosity (cP)	Ref.
Canada	East Bodo	29,000	NR	417–2000	HPAM(F3630/F3830)	1500	50–60	[271]
		25,00–27,000	27	600–2000	Associative polymer	1750	30–80	[272]
	Pelican Lake	6853	23	1000–3000	HPAM (13.6 MDa)	600–3000	13–50	[273]
	Mooney	28,700	29	300–1000	Associative polymer	2200	NR	[272]
China	SZ36-1	6071	65	70	Associative polymer	600–2400	98	[274]
	Daqing	6000	45	10–30	HPAM	1000–2500	40–300	[275,276]
	Shengtuo	21,000	80	10–40	HPAM	1800	30–50	[261]
	Bohai Bay	2873– 20,000	50–70	30–450	HPAM	1200–2500	98	[277]
		6071–9347	65	24–452	Associative polymer (AP-P4)	1750	131	[278]
	Gudao	8207	65	50–150	HPAM	2000	350	[261]
	ShuangHe	5060	72	7.8	HPAM	1090	93	[279]
Brazil	Buracica	41,000	60	7–20	HPAM (Flopam)	500	10	[280]
	Carmopolis	17,091	50	10.5	HPAM (Flopam)	500	40	[281]
Oman	Marmul	3000	46	80–90	HPAM (Nalco Q41F)	1000	15	[282,283]
Suriname	Tambaredjo	5000	38	325–2209	HPAM (3630S)	1000–2500	45–140	[284]
India	Mangala	5400	62	9–22	HPAM	2000–2500	20	[285,286]
Germany	Bockstedt	186,000	54	11–29	Schizophyllan	300	25	[268,269]
Angola	Dalia/Camelia	117,700	45–56	1–11	HPAM (18–20 MDa)	900	3	[263,264]

8. Final Remarks

Polymer flooding is a mature enhanced oil recovery technique that has proven to be successful in field applications over the past 50 years. In recent years, there has been growing interest in the application of water-soluble polymers for field projects. This is because of the development of advanced polymers for high-salinity and high-temperature conditions and an improved understanding of the flow mechanisms of polymers in porous media. In this review, we attempted to give an overview of the latest research progress in the application of water-soluble polymers for cEOR. However, there are other challenges that currently exist in field applications. They include injectivity decline at low-permeability formations, long-term stability at high-salinity and high-temperature conditions, and the need for cost-effective and environmentally friendly polymers. Further review of such topics is recommended to ensure a successful implementation of the technology.

9. Summary and Outlook

In this review, we presented a critical overview of the state-of-the-art research on water-soluble polymers for cEOR. The objective of this review was to revisit the fundamentals of polymer flow in porous media and to present the recent progress made in (a) the improved understanding of the flow behavior of water-soluble polymers in porous media (e.g., shear thickening, elastic turbulence) and (b) the development of advanced water-soluble polymers for enhanced oil recovery at high-salinity and high-temperature conditions and their use in field applications.

Polymers can improve oil recovery by increasing the viscosity of the aqueous phase, thus reducing the mobility ratio. More recently, the improvement in oil recovery by polymers is also attributed to their viscoelastic properties, due to which polymers can displace the residual oil trapped by capillary forces. As a result of the flow of a viscoelastic polymer in porous media, fluctuating pressure fields are generated, which destabilizes the trapped oil ganglia and improves the oil recovery.

One of the most debated flow behaviors that is related to the viscoelastic nature of a polymer solution in porous media, is the shear-thickening behavior. Shear thickening has previously been explained by the coil–stretch transition and transient network theories and more recently attributed to elastic instabilities at negligible inertial effect. Beyond the onset of these elastic instabilities, the flow shows strong spatiotemporal fluctuations and causes viscous dissipation which results in the anomalous increase in the apparent viscosity.

The performance of polymers in porous media (i.e., polymer rheology and retention) is dependent on many parameters, including polymer type, polymer molecular weight and concentration, porous media permeability, residual oil saturation, iron and clay content of the rock, salinity, and temperature. The employment of conventional polymers at high-salinity and high-temperature reservoirs is a challenge and there is limited success in field applications. The modification of polyacrylamide hydrophobically or with monomers such as AMPS and N-VP has shown promising results at high-temperature and high-salinity conditions; however, these polymers are more expensive than conventional polymers used for cEOR such as HPAM.

An alternative approach for achieving enhanced stability and high viscosity at high-salinity and high-temperature conditions is combining polymers with silica nanoparticles. The rheological properties of such a system can be controlled by finetuning the interactions between polymers and nanoparticles. As a result, a molecular network structure with a larger hydrodynamic volume will be formed, which in turn results in an increase in the polymer solution viscosity. Despite success at high-salinity and high-temperature conditions in the short term, the long-term stability for the polymer–nanoparticles hybrid can be more challenging, since silica nanoparticles can partially lose their surface functionalities at high temperatures in the long term, which can lead to their aggregation and injectivity problems.

Author Contributions: M.M.Y. contributed to obtaining the pieces of the literature and drafting the manuscript; P.E.B. and P.Z. also contributed to obtaining the pieces of the literature and made important suggestions and recommendations for the paper review. All authors have read and agreed to the published version of the manuscript.

Funding: This research received no external funding.

Acknowledgments: Sian Jones is greatly acknowledged for proofreading this paper.

Conflicts of Interest: The authors declare no conflict of interest.

References

1. BP Energy Outlook. 2019. Available online: https://www.bp.com/content/dam/bp/business-sites/en/global/corporate/pdfs/energy-economics/energy-outlook/bp-energy-outlook-2019.pdf (accessed on 1 January 2020).
2. Sandrea, I.; Sandrea, R. Global oil reserves—1: Recovery factors leave vast target for EOR technologies. *Oil Gas J.* **2007**, *105*, 44–48.
3. Muggeridge, A.; Cockin, A.; Webb, K.; Frampton, H.; Collins, I.; Moulds, T.; Salino, P. Recovery rates, enhanced oil recovery and technological limits. *Philos. Trans. R. Soc. A Math. Phys. Eng. Sci.* **2013**, *372*, 20120320. [CrossRef] [PubMed]

4. Lake, L.; Johns, R.T.; Rossen, W.R.; Pope, G.A. *Fundamentals of Enhanced Oil Recovery*; Society of Petroleum Engineers: Richardson, TX, USA, 2014.
5. Sorbie, K.S. Network Modeling of Xanthan Rheology in Porous Media in the Presence of Depleted Layer Effects. In Proceedings of the SPE Annual Technical Conference and Exhibition, San Antonio, TX, USA, 1 January 1989; p. 14.
6. Sheng, J. *Modern Chemical Enhanced Oil Recovery: Theory and Practice*; Gulf Professional Publishing: Huston, TX, USA, 2010.
7. Yegane, M.M.; Ayatollahi, S.; Bashtani, F.; Romero, C. Solar Generated Steam Injection in Hamca, Venezuelan Extra Heavy Oil Reservoir; Simulation Study for Oil Recovery Performance, Economical and Environmental Feasibilities. In Proceedings of the EUROPEC 2015, Madrid, Spain, 1–4 June 2015; p. 27.
8. Yegane, M.M.; Bashtani, F.; Tahmasebi, A.; Ayatollahi, S.; Al-wahaibi, Y.M. Comparing Different Scenarios for Thermal Enhanced Oil Recovery in Fractured Reservoirs Using Hybrid (Solar-Gas) Steam Generators, A Simulation Study. In Proceedings of the SPE Europec featured at 78th EAGE Conference and Exhibition, Vienna, Austria, 30 May 2016; p. 19.
9. Mirzaie Yegane, M.; Battistutta, E.; Zitha, P. Mechanistic Simulation and History Matching of Alkaline-Surfactant-Polymer ASP Core Flooding Experiment at Optimum vs. Under-Optimum Salinity Conditions. In Proceedings of the SPE Europec Featured at 81st EAGE Conference and Exhibition, London, UK, 3–6 June 2019; p. 22.
10. Pye, D.J. Improved Secondary Recovery by Control of Water Mobility. *J. Pet. Technol.* **1964**, *16*, 911–916. [CrossRef]
11. Sandiford, B.B. Laboratory and Field Studies of Water Floods Using Polymer Solutions to Increase Oil Recoveries. *J. Pet. Technol.* **1964**, *16*, 917–922. [CrossRef]
12. Chang, H.L. Polymer Flooding Technology Yesterday, Today, and Tomorrow. *J. Pet. Technol.* **1978**, *30*, 1113–1128. [CrossRef]
13. Jewett, R.L.; Schurz, G.F. Polymer Flooding-A Current Appraisal. *J. Pet. Technol.* **1970**, *22*, 675–684. [CrossRef]
14. Needham, R.B.; Doe, P.H. Polymer Flooding Review. *J. Pet. Technol.* **1987**, *39*, 1503–1507. [CrossRef]
15. Du, Y.; Guan, L. Field-scale Polymer Flooding: Lessons Learnt and Experiences Gained During Past 40 Years. In Proceedings of the SPE International Petroleum Conference in Mexico, Puebla Pue, Mexico, 7–9 November 2004; p. 6.
16. Manrique, E.J.; Thomas, C.P.; Ravikiran, R.; Izadi Kamouei, M.; Lantz, M.; Romero, J.L.; Alvarado, V. EOR: Current Status and Opportunities. In Proceedings of the SPE Improved Oil Recovery Symposium, Tulsa, OK, USA, 24–28 April 2010; p. 21.
17. Corlay, P.; Lemouzy, P.; Eschard, R.; Zhang, L.R. Fully Integrated Reservoir Study and Numerical Forecast Simulations of Two-Polymer Pilots in Daqing Field. In Proceedings of the International Meeting on Petroleum Engineering, Beijing, China, 24–27 March 1992; p. 10.
18. Wang, D.; Cheng, J.; Wu, J.; Wang, Y. Producing by Polymer Flooding more than 300 Million Barrels of Oil, What Experiences Have Been Learnt? In Proceedings of the SPE Asia Pacific Oil and Gas Conference and Exhibition, Melbourne, Australia, 8–10 October 2002; p. 9.
19. Wang, D.; Wang, G.; Xia, H.; Yang, S.; Wu, W. Incremental Recoveries in the Field of Large Scale High Viscous-Elastic Fluid Flooding are Double that of Conventional Polymer Flooding. In Proceedings of the SPE Annual Technical Conference and Exhibition, Denver, CO, USA, 30 October–2 November 2011; p. 14.
20. Yang, F.; Wang, D.; Yang, X.; Sui, X.; Chen, Q.; Zhang, L. High Concentration Polymer Flooding is Successful. In Proceedings of the SPE Asia Pacific Oil and Gas Conference and Exhibition, Perth, Australia, 18–20 October 2004; p. 7.
21. Needham, R.B.; Threlkeld, C.B.; Gall, J.W. Control of Water Mobility Using Polymers and Multivalent Cations. In Proceedings of the SPE Improved Oil Recovery Symposium, Tulsa, OK, USA, 22–24 April 1974; p. 10.
22. Standnes, D.C.; Skjevrak, I. Literature review of implemented polymer field projects. *J. Pet. Sci. Eng.* **2014**, *122*, 761–775. [CrossRef]
23. Mohsenatabar Firozjaii, A.; Saghafi, H.R. Review on chemical enhanced oil recovery using polymer flooding: Fundamentals, experimental and numerical simulation. *Petroleum* **2019**, *6*, 115–122. [CrossRef]
24. Rellegadla, S.; Prajapat, G.; Agrawal, A. Polymers for enhanced oil recovery: Fundamentals and selection criteria. *Appl. Microbiol. Biotechnol.* **2017**, *101*, 4387–4402. [CrossRef]
25. Wever, D.A.Z.; Picchioni, F.; Broekhuis, A.A. Polymers for enhanced oil recovery: A paradigm for structure–property relationship in aqueous solution. *Prog. Polym. Sci.* **2011**, *36*, 1558–1628. [CrossRef]
26. Kamal, M.S.; Sultan, A.S.; Al-Mubaiyedh, U.A.; Hussein, I.A. Review on Polymer Flooding: Rheology, Adsorption, Stability, and Field Applications of Various Polymer Systems. *Polym. Rev.* **2015**, *55*, 491–530. [CrossRef]
27. Thomas, A.; Gaillard, N.; Favero, C. Some Key Features to Consider When Studying Acrylamide-Based Polymers for Chemical Enhanced Oil Recovery. *Oil Gas Sci. Technol.-Rev. D'ifp Energ. Nouv.* **2012**, *67*, 887–902. [CrossRef]
28. Scott, A.J.; Romero-Zerón, L.; Penlidis, A. Evaluation of Polymeric Materials for Chemical Enhanced Oil Recovery. *Processes* **2020**, *8*, 361. [CrossRef]
29. Al-Hajri, S.; Mahmood, S.M.; Abdulelah, H.; Akbari, S. An Overview on Polymer Retention in Porous Media. *Energies* **2018**, *11*, 2751. [CrossRef]
30. Weiss, W.W.; Baldwin, R.W. Planning and implementing a large-scale polymer flood. *J. Pet. Technol.* **1985**, *37*, 720–730. [CrossRef]
31. Skauge, A.; Zamani, N.; Gausdal Jacobsen, J.; Shaker Shiran, B.; Al-Shakry, B.; Skauge, T. Polymer Flow in Porous Media: Relevance to Enhanced Oil Recovery. *Colloids Interfaces* **2018**, *2*, 27. [CrossRef]
32. Abidin, A.Z.; Puspasari, T.; Nugroho, W.A. Polymers for Enhanced Oil Recovery Technology. *Procedia Chem.* **2012**, *4*, 11–16. [CrossRef]

33. Alfazazi, U.; AlAmeri, W.; Hashmet, M.R. Screening of New HPAM Base Polymers for Applications in High Temperature and High Salinity Carbonate Reservoirs. In Proceedings of the Abu Dhabi International Petroleum Exhibition & Conference, Abu Dhabi, United Arab Emirates, 5–8 October 2008.
34. Chauveteau, G. Fundamental Criteria in Polymer Flow Through Porous Media. In *Water-Soluble Polymers*; Advances in Chemistry; American Chemical Society: Washington, DC, USA, 1986; Volume 213, pp. 227–267.
35. Kheradmand, H.; François, J.; Plazanet, V. Hydrolysis of polyacrylamide and acrylic acid-acrylamide copolymers at neutral pH and high temperature. *Polymer* **1988**, *29*, 860–870. [CrossRef]
36. Ash, S.G.; Clarke-Sturman, A.J.; Calvert, R.; Nisbet, T.M. Chemical Stability of Biopolymer Solutions. In Proceedings of the SPE Annual Technical Conference and Exhibition, San Francisco, CA, USA, 5–8 October 2008; p. 8.
37. Cadmus, M.C.; Jackson, L.K.; Burton, K.A.; Plattner, R.D.; Slodki, M.E. Biodegradation of Xanthan Gum by *Bacillus* sp. *Appl. Environ. Microbiol.* **1982**, *44*, 5–11. [CrossRef]
38. Schulz, D.N.; Kaladas, J.J.; Maurer, J.J.; Bock, J.; Pace, S.J.; Schulz, W.W. Copolymers of acrylamide and surfactant macromonomers: Synthesis and solution properties. *Polymer* **1987**, *28*, 2110–2115. [CrossRef]
39. Senan, C.; Meadows, J.; Shone, P.T.; Williams, P.A. Solution Behavior of Hydrophobically Modified Sodium Polyacrylate. *Langmuir* **1994**, *10*, 2471–2479. [CrossRef]
40. Durand, A.; Hourdet, D. Synthesis and thermoassociative properties in aqueous solution of graft copolymers containing poly(N-isopropylacrylamide) side chains. *Polymer* **1999**, *40*, 4941–4951. [CrossRef]
41. Levitt, D.; Pope, G.A. Selection and Screening of Polymers for Enhanced-Oil Recovery. In Proceedings of the SPE Symposium on Improved Oil Recovery, Tulsa, OK, USA, 20–23 April 2008; p. 18.
42. Doe, P.H.; Moradi-Araghi, A.; Shaw, J.E.; Stahl, G.A. Development and Evaluation of EOR Polymers Suitable for Hostile Environments Part 1: Copolymers of Vinylpyrrolidone and Acrylamide. *SPE Reserv. Eng.* **1987**, *2*, 461–467. [CrossRef]
43. Wei, B.; Romero-Zerón, L.; Rodrigue, D. Oil displacement mechanisms of viscoelastic polymers in enhanced oil recovery (EOR): A review. *J. Pet. Explor. Prod. Technol.* **2014**, *4*, 113–121. [CrossRef]
44. Al-Shakry, B.; Skauge, T.; Shaker Shiran, B.; Skauge, A. Impact of Mechanical Degradation on Polymer Injectivity in Porous Media. *Polymers* **2018**, *10*, 742. [CrossRef]
45. Vermolen, E.C.; Haasterecht, M.J.; Masalmeh, S.K. A Systematic Study of the Polymer Visco-Elastic Effect on Residual Oil Saturation by Core Flooding. In Proceedings of the SPE EOR Conference at Oil and Gas West Asia, Muscat, Oman, 31 March–2 April 2014.
46. Clarke, A.; Howe, A.M.; Mitchell, J.; Staniland, J.; Hawkes, L.A. How Viscoelastic-Polymer Flooding Enhances Displacement Efficiency. *SPE J.* **2016**, *21*, 0675–0687. [CrossRef]
47. Emami Meybodi, H.; Kharrat, R.; Wang, X. Study of Microscopic and Macroscopic Displacement Behaviors of Polymer Solution in Water-Wet and Oil-Wet Media. *Transp. Porous Media* **2011**, *89*, 97–120. [CrossRef]
48. Mahajan, S.; Yadav, H.; Rellegadla, S.; Agrawal, A. Polymers for enhanced oil recovery: Fundamentals and selection criteria revisited. *Appl. Microbiol. Biotechnol.* **2021**, *105*, 8073–8090. [CrossRef]
49. Rock, A.; Hincapie, R.E.; Tahir, M.; Langanke, N.; Ganzer, L. On the Role of Polymer Viscoelasticity in Enhanced Oil Recovery: Extensive Laboratory Data and Review. *Polymers* **2020**, *12*, 2276. [CrossRef]
50. Han, X.; Li, C.; Pan, F.; Li, Y.; Feng, Y. A comparative study on enhancing oil recovery with partially hydrolyzed polyacrylamide: Emulsion versus powder. *Can. J. Chem. Eng.* **2022**, *100*, 1336–1348. [CrossRef]
51. Gbadamosi, A.O.; Junin, R.; Manan, M.A.; Agi, A.; Yusuff, A.S. An overview of chemical enhanced oil recovery: Recent advances and prospects. *International Nano Letters* **2019**, *9*, 171–202. [CrossRef]
52. Sorbie, K.S. *Polymer-Improved Oil Recovery*; Springer: Dordrecht, The Netherlands, 1991.
53. Hu, Y.; Wang, S.Q.; Jamieson, A.M. Rheological and Rheooptical Studies of Shear-Thickening Polyacrylamide Solutions. *Macromolecules* **1995**, *28*, 1847–1853. [CrossRef]
54. Kawale, D.; Marques, E.; Zitha, P.L.J.; Kreutzer, M.T.; Rossen, W.R.; Boukany, P.E. Elastic instabilities during the flow of hydrolyzed polyacrylamide solution in porous media: Effect of pore-shape and salt. *Soft Matter* **2017**, *13*, 765–775. [CrossRef] [PubMed]
55. Portehault, D.; Petit, L.; Hourdet, D. Synthesis and self assembly processes of aqueous thermoresponsive hybrid formulations. *Soft Matter* **2010**, *6*, 2178–2186. [CrossRef]
56. Green, D.W.; Willhite, G.P. *Enhanced Oil Recovery*; Society of Petroleum Engineers: Richardson, TX, USA, 1998.
57. Doda, A.; Azad, M.S.; Trivedi, J.J. Effect of water saturation on the role of polymer elasticity during heavy oil recovery. *J. Dispers. Sci. Technol.* **2020**, *41*, 1265–1273. [CrossRef]
58. Schneider, F.N.; Owens, W.W. Steady-State Measurements of Relative Permeability for Polymer/Oil Systems. *Soc. Pet. Eng. J.* **1982**, *22*, 79–86. [CrossRef]
59. Taber, J.J. Technical Screening Guides for the Enhanced Recovery of Oil. In Proceedings of the SPE Annual Technical Conference and Exhibition, San Francisco, CA, USA, 5–8 October 1983; p. 20.
60. Mennella, A.; Chiappa, L.; Bryant, S.L.; Burrafato, G. Pore-scale Mechanism for Selective Permeability Reduction by Polymer Injection. In Proceedings of the SPE/DOE Improved Oil Recovery Symposium, Tulsa, OK, USA, 19–22 April 1998; p. 12.
61. Liang, J.-T.; Seright, R.S. Further Investigations of Why Gels Reduce Water Permeability More Than Oil Permeability. *SPE Prod. Facil.* **1997**, *12*, 225–230. [CrossRef]

62. Liang, B.; Jiang, H.; Li, J.; Chen, F.; Miao, W.; Yang, H.; Qiao, Y.; Chen, W. Mechanism Study of Disproportionate Permeability Reduction Using Nuclear Magnetic Resonance T2. *Energy Fuels* **2018**, *32*, 4959–4968. [CrossRef]
63. Ye, Z.; He, E.; Xie, S.; Han, L.; Chen, H.; Luo, P.; Shu, Z.; Shi, L.; Lai, N. The mechanism study of disproportionate permeability reduction by hydrophobically associating water-soluble polymer gel. *J. Pet. Sci. Eng.* **2010**, *72*, 64–66. [CrossRef]
64. Barreau, P.; Bertin, H.; Lasseux, D.; Glénat, P.; Zaitoun, A. Water Control in Producing Wells: Influence of an Adsorbed-Polymer Layer on Relative Permeabilities and Capillary Pressure. *SPE Reserv. Eng.* **1997**, *12*, 234–239. [CrossRef]
65. Zaitoun, A.; Kohler, N. Two-Phase Flow Through Porous Media: Effect of an Adsorbed Polymer Layer. In Proceedings of the SPE Annual Technical Conference and Exhibition, Houston, TX, USA, 21–22 May 2001; p. 14.
66. Wu, Q.; Ge, J.; Ding, L.; Guo, H.; Wang, W.; Fan, J. Insights into the key aspects influencing the rheological properties of polymer gel for water shutoff in fractured reservoirs. *Colloids Surf. A Physicochem. Eng. Asp.* **2022**, *634*, 127963. [CrossRef]
67. Wang, D.; Cheng, J.; Yang, Q.; Wenchao, G.; Qun, L.; Chen, F. Viscous-Elastic Polymer Can Increase Microscale Displacement Efficiency in Cores. In Proceedings of the SPE Annual Technical Conference and Exhibition, Dallas, TX, USA, 1–4 October 2000; p. 10.
68. Hou, J.; Li, Z.; Zhang, S.; Cao, X.; Du, Q.; Song, X. Computerized Tomography Study of the Microscopic Flow Mechanism of Polymer Flooding. *Transp. Porous Media* **2009**, *79*, 407–418. [CrossRef]
69. Wang, D.; Wang, G.; Wu, W.; Xia, H.; Yin, H. The Influence of Viscoelasticity on Displacement Efficiency—From Micro- to Macroscale. In Proceedings of the SPE Annual Technical Conference and Exhibition, Anaheim, CA, USA, 11–14 November 2007; p. SPE-109016-MS.
70. Luo, D.; Wang, F.; Zhu, J.; Cao, F.; Liu, Y.; Li, X.; Willson, R.C.; Yang, Z.; Chu, C.-W.; Ren, Z. Nanofluid of graphene-based amphiphilic Janus nanosheets for tertiary or enhanced oil recovery: High performance at low concentration. *Proc. Natl. Acad. Sci. USA* **2016**, *113*, 7711–7716. [CrossRef] [PubMed]
71. Delshad, M.; Kim, D.H.; Magbagbeola, O.A.; Huh, C.; Pope, G.A.; Tarahhom, F. Mechanistic Interpretation and Utilization of Viscoelastic Behavior of Polymer Solutions for Improved Polymer-Flood Efficiency. In Proceedings of the SPE Symposium on Improved Oil Recovery, Tulsa, OK, USA, 20–23 April 2008; p. SPE-113620-MS.
72. Khalilinezhad, S.S.; Hashemi, A.; Mobaraki, S.; Zakavi, M.; Jarrahian, K. Experimental Analysis and Numerical Modeling of Polymer Flooding in Heavy Oil Recovery Enhancement: A Pore-Level Investigation. *Arab. J. Sci. Eng.* **2019**, *44*, 10447–10465. [CrossRef]
73. Yakimchuk, I.; Evseev, N.; Korobkov, D.; Ridzel, O.; Pletneva, V.; Yaryshev, M.; Ilyasov, I.; Glushchenko, N.; Orlov, A. Study of Polymer Flooding at Pore Scale by Digital Core Analysis for East-Messoyakhskoe Oil Field. In Proceedings of the SPE Russian Petroleum Technology Conference, Virtual, 26–29 October 2020; p. D043S020R001.
74. Xie, C.; Qi, P.; Xu, K.; Xu, J.; Balhoff, M.T. Oscillative Trapping of a Droplet in a Converging Channel Induced by Elastic Instability. *Phys. Rev. Lett.* **2022**, *128*, 054502. [CrossRef]
75. Xie, C.; Xu, K.; Mohanty, K.; Wang, M.; Balhoff, M.T. Nonwetting droplet oscillation and displacement by viscoelastic fluids. *Phys. Rev. Fluids* **2020**, *5*, 063301. [CrossRef]
76. Erincik, M.Z.; Qi, P.; Balhoff, M.T.; Pope, G.A. New Method To Reduce Residual Oil Saturation by Polymer Flooding. *SPE J.* **2018**, *23*, 1944–1956. [CrossRef]
77. Qi, P.; Ehrenfried, D.H.; Koh, H.; Balhoff, M.T. Reduction of Residual Oil Saturation in Sandstone Cores by Use of Viscoelastic Polymers. *SPE J.* **2017**, *22*, 447–458. [CrossRef]
78. McKinley, G.H.; Pakdel, P.; Öztekin, A. Rheological and geometric scaling of purely elastic flow instabilities. *J. Non-Newton. Fluid Mech.* **1996**, *67*, 19–47. [CrossRef]
79. Clarke, A.; Howe, A.M.; Mitchell, J.; Staniland, J.; Hawkes, L.; Leeper, K. Mechanism of anomalously increased oil displacement with aqueous viscoelastic polymer solutions. *Soft Matter* **2015**, *11*, 3536–3541. [CrossRef] [PubMed]
80. Moan, M.; Chauveteau, G.; Ghoniem, S. Entrance effect in capillary flow of dilute and semi-dilute polymer solutions. *J. Non-Newton. Fluid Mech.* **1979**, *5*, 463–474. [CrossRef]
81. Chauveteau, G.; Moan, M.; Magueur, A. Thickening behaviour of dilute polymer solutions in non-inertial elongational flows. *J. Non-Newton. Fluid Mech.* **1984**, *16*, 315–327. [CrossRef]
82. Hoa, N.T.C.G.; Gaudu, R.; Anne-Archard, D. Relation entre le champ de vitesse d'elongation et l'apparition d'un comportement dilatant d'une solution de polymere diluee dans un ecoulement convergent non-inertiel. *C. R. Acad. Sci. Paris* **1982**, *294*, 927.
83. Mirzaie Yegane, M.; Schmidt, J.; Dugonjic-Bilic, F.; Gerlach, B.; Boukany, P.E.; Zitha, P.L.J. Flow Enhancement of Water-Soluble Polymers through Porous Media by Preshearing. *Ind. Eng. Chem. Res.* **2021**, *60*, 3463–3473. [CrossRef]
84. Schmidt, J.; Mirzaie Yegane, M.; Dugonjic-Bilic, F.; Gerlach, B.; Zitha, P. Novel Method For Mitigating Injectivity Issues During Polymer Flooding at High Salinity Conditions. In Proceedings of the SPE Europec Featured at 81st EAGE Conference and Exhibition, London, UK, 3–6 June 2019.
85. Salmo, I.C.; Sorbie, K.S.; Skauge, A. The Impact of Rheology on Viscous Oil Displacement by Polymers Analyzed by Pore-Scale Network Modelling. *Polymers* **2021**, *13*, 1259. [CrossRef]
86. Stavland, A.; Jonsbraten, H.; Lohne, A.; Moen, A.; Giske, N.H. Polymer Flooding—Flow Properties in Porous Media versus Rheological Parameters. In Proceedings of the SPE EUROPEC/EAGE Annual Conference and Exhibition, Barcelona, Spain, 14–17 June 2010; p. 15.
87. Kawale, D.; Bouwman, G.; Sachdev, S.; Zitha, P.L.J.; Kreutzer, M.T.; Rossen, W.R.; Boukany, P.E. Polymer conformation during flow in porous media. *Soft Matter* **2017**, *13*, 8745–8755. [CrossRef]

88. Tahir, M.; Hincapie, R.E.; Ganzer, L. An Elongational and Shear Evaluation of Polymer Viscoelasticity during Flow in Porous Media. *Appl. Sci.* **2020**, *10*, 4152. [CrossRef]
89. Browne, C.A.; Shih, A.; Datta, S.S. Pore-Scale Flow Characterization of Polymer Solutions in Microfluidic Porous Media. *Small* **2020**, *16*, 1903944. [CrossRef]
90. Chauveteau, G.; Moan, M. The onset of dilatant behaviour in non-inertial flow of dilute polymer solutions through channels with varying cross-sections. *J. Phys. Lett.* **1981**, *42*, 201–204. [CrossRef]
91. Flew, S.; Sellin, R.H.J. Non-Newtonian flow in porous media-a laboratory study of polyacrylamide solutions. *J. Non-Newton. Fluid Mech.* **1993**, *47*, 169–210. [CrossRef]
92. Durst, F.; Haas, R.; Interthal, W. The nature of flows through porous media. *J. Non-Newton. Fluid Mech.* **1987**, *22*, 169–189. [CrossRef]
93. Haas, R.; Durst, F. Viscoelastic flow of dilute polymer solutions in regularly packed beds. *Rheol. Acta* **1982**, *21*, 566–571. [CrossRef]
94. Gennes, P.G.D. Coil-stretch transition of dilute flexible polymers under ultrahigh velocity gradients. *J. Chern. Phys.* **1974**, *60*, 5030–5042. [CrossRef]
95. Zimm, B.H. Dynamics of Polymer Molecules in Dilute Solution: Viscoelasticity, Flow Birefringence and Dielectric Loss. *J. Chern. Phys.* **1956**, *24*, 269–278. [CrossRef]
96. Larson, R.G.; Magda, J.J. Coil-stretch transitions in mixed shear and extensional flows of dilute polymer solutions. *Macromolecules* **1989**, *22*, 3004–3010. [CrossRef]
97. Perkins, T.T.; Smith, D.E.; Chu, S. Single Polymer Dynamics in an Elongational Flow. *Science* **1997**, *276*, 2016. [CrossRef]
98. Shaqfeh, E.S.G. The dynamics of single-molecule DNA in flow. *J. Non-Newton. Fluid Mech.* **2005**, *130*, 1–28. [CrossRef]
99. Sachdev, S.; Muralidharan, A.; Boukany, P.E. Molecular Processes Leading to "Necking" in Extensional Flow of Polymer Solutions: Using Microfluidics and Single DNA Imaging. *Macromolecules* **2016**, *49*, 9578–9585. [CrossRef]
100. Odell, J.; Müller, A.; Keller, A. Non-Newtonian Behaviour of Hydrolysed Polyacrylamide in Strong Elongational Flows: A Transient Network Approach. *Polymer* **1988**, *29*, 1179–1190. [CrossRef]
101. Wang, S.Q. Transient network theory for shear-thickening fluids and physically crosslinked networks. *Macromolecules* **1992**, *25*, 7003–7010. [CrossRef]
102. Galindo-Rosales, F.; Campo-Deaño, L.; Pinho, F.; van Bokhorst, E.; Hamersma, P.; Oliveira, M.; Alves, M. Microfluidic systems for the analysis of viscoelastic fluid flow phenomena in porous media. *Microfluid. Nanofluidics* **2011**, *12*, 485–498. [CrossRef]
103. Howe, A.M.; Clarke, A.; Giernalczyk, D. Flow of concentrated viscoelastic polymer solutions in porous media: Effect of MW and concentration on elastic turbulence onset in various geometries. *Soft Matter* **2015**, *11*, 6419–6431. [CrossRef] [PubMed]
104. Machado, A.; Bodiguel, H.; Beaumont, J.; Clisson, G.; Colin, A. Extra dissipation and flow uniformization due to elastic instabilities of shear-thinning polymer solutions in model porous media. *Biomicrofluidics* **2016**, *10*, 043507. [CrossRef] [PubMed]
105. Browne, C.A.; Datta, S.S. Elastic turbulence generates anomalous flow resistance in porous media. *Sci. Adv.* **2021**, *7*, eabj2619. [CrossRef]
106. Müller, A.; Sáez, A. *The Rheology of Polymer Solutions in Porous Media*; Springer: Berlin/Heidelberg, Germany, 1999; pp. 335–393.
107. Sadowski, T.J. Non-Newtonian Flow through Porous Media. II. Experimental. *Trans. Soc. Rheol.* **1965**, *9*, 251–271. [CrossRef]
108. Sorbie, K.S.; Clifford, P.J.; Jones, E.R.W. The rheology of pseudoplastic fluids in porous media using network modeling. *J. Colloid Interface Sci.* **1989**, *130*, 508–534. [CrossRef]
109. Pearson, J.R.A.; Tardy, P.M.J. Models for flow of non-Newtonian and complex fluids through porous media. *J. Non-Newton. Fluid Mech.* **2002**, *102*, 447–473. [CrossRef]
110. Lopez, X.; Valvatne, P.H.; Blunt, M.J. Predictive network modeling of single-phase non-Newtonian flow in porous media. *J. Colloid Interface Sci.* **2003**, *264*, 256–265. [CrossRef]
111. Savins, J.G. Non-newtonian flow through porous media. *Ind. Eng. Chem.* **1969**, *61*, 18–47. [CrossRef]
112. Sochi, T. Non-Newtonian flow in porous media. *Polymer* **2010**, *51*, 5007–5023. [CrossRef]
113. Shenoy, A.V. Darcy-Forchheimer natural, forced and mixed convection heat transfer in non-Newtonian power-law fluid-saturated porous media. *Transp. Porous Media* **1993**, *11*, 219–241. [CrossRef]
114. Schümmer, P. Mechanics of Non-Newtonian Fluids. Von W. R. Schowalter. Pergamon Press, Oxford–Frankfurt 1978. 1. Aufl., IX, 300 S., zahlr. Abb. u. Tab., geb., $35.00. *Chem. Ing. Tech.* **1979**, *51*, 766. [CrossRef]
115. McCabe, W.L.; Smith, J.C.; Harriott, P. *Unit Operations of Chemical Engineering*, 7th ed.; McGraw-Hill Education: New York, NY, USA, 2004; 1168p.
116. Scheidegger, A.E. Theoritical models of porous matter. *Producers Monthly (August)*, 1953; pp. 17–23.
117. Sadowski, T.J.; Bird, R.B. Non-Newtonian Flow through Porous Media. I. Theoretical. *Trans. Soc. Rheol.* **1965**, *9*, 243–250. [CrossRef]
118. Duda, J.L.; Hong, S.A.; Klaus, E.E. Flow of polymer solutions in porous media: Inadequacy of the capillary model. *Ind. Eng. Chem. Fundam.* **1983**, *22*, 299–305. [CrossRef]
119. Dullien, F.A.L. 1—Pore Structure. In *Porous Media*, 2nd ed.; Dullien, F.A.L., Ed.; Academic Press: San Diego, CA, USA, 1992; pp. 5–115.
120. Sochi, T. Pore-Scale Modeling of Non-Newtonian Flow in Porous Media. *arXiv* **2010**, arXiv:1011.0760.
121. Xie, C.; Balhoff, M.T. Lattice Boltzmann Modeling of the Apparent Viscosity of Thinning–Elastic Fluids in Porous Media. *Transp. Porous Media* **2021**, *137*, 63–86. [CrossRef]

122. Xie, C.; Lv, W.; Wang, M. Shear-thinning or shear-thickening fluid for better EOR?—A direct pore-scale study. *J. Pet. Sci. Eng.* **2018**, *161*, 683–691. [CrossRef]
123. Xie, C.; Lei, W.; Wang, M. Lattice Boltzmann model for three-phase viscoelastic fluid flow. *Phys. Rev. E* **2018**, *97*, 023312. [CrossRef]
124. Willhite, G.P.; Dominguez, J.G. Mechanisms of polymer retention in porous media. In *Improved Oil Recovery by Surfactant and Polymer Flooding*; Shah, D.O., Schechter, R.S., Eds.; Academic Press: Cambridge, MA, USA, 1977; pp. 511–554.
125. Gogarty, W.B. Mobility Control With Polymer Solutions. *Soc. Pet. Eng. J.* **1967**, *7*, 161–173. [CrossRef]
126. Szabo, M.T. Some Aspects of Polymer Retention in Porous Media Using a C14-Tagged Hydrolyzed Polyacrylamide. *Soc. Pet. Eng. J.* **1975**, *15*, 323–337. [CrossRef]
127. Marker, J.M. Dependence of Polymer Retention on Flow Rate. *J. Pet. Technol.* **1973**, *25*, 1307–1308. [CrossRef]
128. Huh, C.; Lange, E.A.; Cannella, W.J. Polymer Retention in Porous Media. In Proceedings of the SPE/DOE Enhanced Oil Recovery Symposium, Tulsa, OK, USA, 22–25 April 1990; p. 20.
129. Stutzmann, T.; Siffert, B. Contribution to the Adsorption Mechanism of Acetamide and Polyacrylamide on to Clays. *Clays Clay Miner.* **1977**, *25*, 392–406. [CrossRef]
130. Pefferkorn, E.; Nabzar, L.; Carroy, A. Adsorption of polyacrylamide to Na kaolinite: Correlation between clay structure and surface properties. *J. Colloid Interface Sci.* **1985**, *106*, 94–103. [CrossRef]
131. Shah, S.; Heinle, S.A.; Glass, J.E. Water-Soluble Polymer Adsorption from Saline Solutions. In Proceedings of the SPE Oilfield and Geothermal Chemistry Symposium, Phoenix, AZ, USA, 9–11 April 1985; p. 10.
132. Lee, J.-J.; Fuller, G.G. Adsorption and desorption of flexible polymer chains in flowing systems. *J. Colloid Interface Sci.* **1985**, *103*, 569–577. [CrossRef]
133. Zitha, P.L.J.; Chauveteau, G.; Léger, L. Unsteady-State Flow of Flexible Polymers in Porous Media. *J. Colloid Interface Sci.* **2001**, *234*, 269–283. [CrossRef]
134. Cohen, Y.; Christ, F.R. Polymer Retention and Adsorption in the Flow of Polymer Solutions Through Porous Media. *SPE Reserv. Eng.* **1986**, *1*, 113–118. [CrossRef]
135. Dawson, R.; Lantz, R.B. Inaccessible Pore Volume in Polymer Flooding. *Soc. Pet. Eng. J.* **1972**, *12*, 448–452. [CrossRef]
136. Liauh, W.C.; Duda, J.L.; Klaus, E.E. *An Investigation of the Inaccessible Pore Volume Phenomena*; Society of Petroleum Engineers: Huston, TX, USA, 1979; Volume 23.
137. DiMarzio, E.A.; Guttman, C.M. Separation by Flow. *Macromolecules* **1970**, *3*, 131–146. [CrossRef]
138. Chauveteau, G.; Kohler, N. Influence of Microgels in Polysaccharide Solutions on Their Flow Behavior Through Porous Media. *Soc. Pet. Eng. J.* **1984**, *24*, 361–368. [CrossRef]
139. Kolodziej, E.J. Mechanism of Microgel Formation in Xanthan Biopolymer Solutions. In Proceedings of the SPE Annual Technical Conference and Exhibition, Dallas, TX, USA, 27–30 September 1987; p. 16.
140. van Domselaar, H.R.; Fortmuller, C. On the Transport Properties of a Rod-Type Polymer in Sand Packs. In Proceedings of the European Petroleum Conference, Cannes, France, 16–18 November 1992; p. 9.
141. Lotsch, T.; Muller, T.; Pusch, G. The Effect of Inaccessible Pore Volume on Polymer Coreflood Experiments. In Proceedings of the SPE Oilfield and Geothermal Chemistry Symposium, Phoenix, AZ, USA, 9–11 April 1985; p. 10.
142. Hughes, D.S.; Teeuw, D.; Cottrell, C.W.; Tollas, J.M. Appraisal of the Use of Polymer Injection to Suppress Aquifer Influx and to Improve Volumetric Sweep in a Viscous Oil Reservoir. *SPE Reserv. Eng.* **1990**, *5*, 33–40. [CrossRef]
143. Osterloh, W.T.; Law, E.J. Polymer Transport and Rheological Properties for Polymer Flooding in the North Sea. In Proceedings of the SPE/DOE Improved Oil Recovery Symposium, Tulsa, OK, USA, 19–22 April 1998; p. 12.
144. UTCHEM Technical Documentation. *Volume II Documentation for UTCHEM 2017_3: A Three-Dimensional Chemical Flood Simulator*; UTCHEM Technical Documentation: Austin, TX, USA, 2017.
145. Seright, R.S. The Effects of Mechanical Degradation and Viscoelastic Behavior on Injectivity of Polyacrylamide Solutions. *Soc. Pet. Eng. J.* **1983**, *23*, 475–485. [CrossRef]
146. Wei, B.; Romero-Zerón, L.; Rodrigue, D. Mechanical Properties and Flow Behavior of Polymers for Enhanced Oil Recovery. *J. Macromol. Sci. Part B* **2014**, *53*, 625–644. [CrossRef]
147. Liang, K.; Han, P.; Chen, Q.; Su, X.; Feng, Y. Comparative Study on Enhancing Oil Recovery under High Temperature and High Salinity: Polysaccharides Versus Synthetic Polymer. *ACS Omega* **2019**, *4*, 10620–10628. [CrossRef]
148. Lakatos, I.; Lakatos-Szabó, J.; Tóth, J. Factors Influencing Polyacrylamide Adsorption in Porous Media and Their Effect on Flow Behavior. In *Surface Phenomena in Enhanced Oil Recovery*; Shah, D.O., Ed.; Springer: Boston, MA, USA, 1981; pp. 821–842.
149. Lecourtier, J.; Lee, L.T.; Chauveteau, G. Adsorption of polyacrylamides on siliceous minerals. *Colloids Surf.* **1990**, *47*, 219–231. [CrossRef]
150. Szabo, M.T. An Evaluation of Water-Soluble Polymers for Secondary Oil Recovery—Parts 1 and 2. *J. Pet. Technol.* **1979**, *31*, 553–570. [CrossRef]
151. Vermolen, E.C.M.; Van Haasterecht, M.J.T.; Masalmeh, S.K.; Faber, M.J.; Boersma, D.M.; Gruenenfelder, M.A. Pushing the envelope for polymer flooding towards high-temperature and high-salinity reservoirs with polyacrylamide based ter-polymers. In Proceedings of the SPE Middle East Oil and Gas Show and Conference, Manama, Bahrain, 25–28 September 2011; p. 9.
152. Dong, H.; Fang, S.; Wang, D.; Wang, J.; Liu, Z.L.; Hou, W. Review of Practical Experience & Management by Polymer Flooding at Daqing. In Proceedings of the SPE Symposium on Improved Oil Recovery, Tulsa, OK, USA, 20–23 April 2008; p. 18.

153. Zhang, X.; Pan, F.; Guan, W.; Li, D.; Li, X.; Guo, S. A Novel Method of Optimizing the Moelcular Weight of Polymer Flooding. In Proceedings of the SPE Enhanced Oil Recovery Conference, Kuala Lumpur, Malaysia, 19–21 July 2011; p. 4.
154. 1Odell, J.A.; Muller, A.J.; Narh, K.A.; Keller, A. Degradation of polymer solutions in extensional flows. *Macromolecules* **1990**, *23*, 3092–3103. [CrossRef]
155. Nguyen, T.Q.; Kausch, H.H. Effects of solvent viscosity on polystyrene degradation in transient elongational flow. *Macromolecules* **1990**, *23*, 5137–5145. [CrossRef]
156. Buchholz, B.A.; Zahn, J.M.; Kenward, M.; Slater, G.W.; Barron, A.E. Flow-induced chain scission as a physical route to narrowly distributed, high molar mass polymers. *Polymer* **2004**, *45*, 1223–1234. [CrossRef]
157. Kuijpers, M.W.A.; Iedema, P.D.; Kemmere, M.F.; Keurentjes, J.T.F. The mechanism of cavitation-induced polymer scission; experimental and computational verification. *Polymer* **2004**, *45*, 6461–6467. [CrossRef]
158. Sivalingam, G.; Agarwal, N.; Madras, G. Distributed midpoint chain scission in ultrasonic degradation of polymers. *AIChE J.* **2004**, *50*, 2258–2265. [CrossRef]
159. Dang, T.Q.C.; Chen, Z.; Nguyen, T.B.N.; Bae, W. Investigation of Isotherm Polymer Adsorption in Porous Media. *Pet. Sci. Technol.* **2014**, *32*, 1626–1640. [CrossRef]
160. Rashidi, M.; Sandvik, S.; Blokhus, A.M.; Skauge, A. Static and Dynamic Adsorption of Salt Tolerant Polymers. In Proceedings of the IOR 2009-15th European Symposium on Improved Oil Recovery, Paris, France, 27–29 April 2009.
161. Lipatov, I.S.; Sergeeva, L.M. *Adsorption of Polymers*; Wiley: Hoboken, NJ, USA, 1974.
162. Gramain, P.; Myard, P. Adsorption studies of polyacrylamides in porous media. *J. Colloid Interface Sci.* **1981**, *84*, 114–126. [CrossRef]
163. Zhang, G.; Seright, R. Effect of Concentration on HPAM Retention in Porous Media. *SPE J.* **2014**, *19*, 373–380. [CrossRef]
164. Deng, Y.; Dixon, J.B.; White, G.N. Adsorption of Polyacrylamide on Smectite, Illite, and Kaolinite. *Soil Sci. Soc. Am. J.* **2006**, *70*, 297–304. [CrossRef]
165. Zheng, C.G.; Gall, B.L.; Gao, H.W.; Miller, A.E.; Bryant, R.S. Effects of Polymer Adsorption and Flow Behavior on Two-Phase Flow in Porous Media. *SPE Reserv. Eval. Eng.* **2000**, *3*, 216–223. [CrossRef]
166. Müller, A.J.; Odell, J.A.; Carrington, S. Degradation of semidilute polymer solutions in elongational flows. *Polymer* **1992**, *33*, 2598–2604. [CrossRef]
167. Smith, F.W. The Behavior of Partially Hydrolyzed Polyacrylamide Solutions in Porous Media. *J. Pet. Technol.* **1970**, *22*, 148–156. [CrossRef]
168. Vela, S.; Peaceman, D.W.; Sandvik, E.I. Evaluation of Polymer Flooding in a Layered Reservoir With Crossflow, Retention, and Degradation. *Soc. Pet. Eng. J.* **1976**, *16*, 82–96. [CrossRef]
169. Seright, R.S. Impact of Permeability and Lithology on Gel Performance. In Proceedings of the SPE/DOE Enhanced Oil Recovery Symposium, Tulsa, OK, USA, 21–24 April 1992; p. 11.
170. Seright, R.S.; Martin, F.D. Impact of Gelation pH, Rock Permeability, and Lithology on the Performance of a Monomer-Based Gel. *SPE Reserv. Eng.* **1993**, *8*, 43–50. [CrossRef]
171. Broseta, D.; Medjahed, F.; Lecourtier, J.; Robin, M. Polymer Adsorption/Retention in Porous Media: Effects of Core Wettability and Residual Oil. *SPE Adv. Technol. Ser.* **1995**, *3*, 103–112. [CrossRef]
172. Kolodziej, E.J. Transport Mechanisms of Xanthan Biopolymer Solutions in Porous Media. In Proceedings of the SPE Annual Technical Conference and Exhibition, Houston, TX, USA, 2–5 October 1988; p. 16.
173. Kottsova, A.K.; Mirzaie Yegane, M.; Tchistiakov, A.A.; Zitha, P.L.J. Effect of electrostatic interaction on the retention and remobilization of colloidal particles in porous media. *Colloids Surf. A Physicochem. Eng. Asp.* **2021**, *617*, 126371. [CrossRef]
174. Sulpizi, M.; Gaigeot, M.-P.; Sprik, M. The Silica–Water Interface: How the Silanols Determine the Surface Acidity and Modulate the Water Properties. *J. Chem. Theory Comput.* **2012**, *8*, 1037–1047. [CrossRef] [PubMed]
175. Tschapek, M. The Point of Zero Charge (pzc) of Kaolinite and SiO2 + Al2O3 Mixtures. *Clay Miner.* **1974**, *10*, 219–229. [CrossRef]
176. Farooq, U.; Tweheyo, M.T.; Sjöblom, J.; Øye, G. Surface Characterization of Model, Outcrop, and Reservoir Samples in Low Salinity Aqueous Solutions. *J. Dispers. Sci. Technol.* **2011**, *32*, 519–531. [CrossRef]
177. Peksa, A.E.; Wolf, K.-H.A.A.; Zitha, P.L.J. Bentheimer sandstone revisited for experimental purposes. *Mar. Pet. Geol.* **2015**, *67*, 701–719. [CrossRef]
178. Gkay, D.H.; Rex, R.W. Formation damage in sandstones caused by clay dispersion and migration. In *Clays and Clay Minerals*; Bailey, S.W., Ed.; Pergamon: Oxford, UK, 1966; pp. 355–366.
179. Simon, D.E.; McDaniel, B.W.; Coon, R.M. Evaluation of Fluid pH Effects on Low Permeability Sandstones. In Proceedings of the SPE Annual Fall Technical Conference and Exhibition, New Orleans, LA, USA, 3–6 October 1976; p. 12.
180. Appel, C.; Ma, L.Q.; Dean Rhue, R.; Kennelley, E. Point of zero charge determination in soils and minerals via traditional methods and detection of electroacoustic mobility. *Geoderma* **2003**, *113*, 77–93. [CrossRef]
181. Dupuis, D.; Lewandowski, F.Y.; Steiert, P.; Wolff, C. Shear thickening and time-dependent phenomena: The case of polyacrylamide solutions. *J. Non-Newton. Fluid Mech.* **1994**, *54*, 11–32. [CrossRef]
182. Peng, S.; Wu, C. Light Scattering Study of the Formation and Structure of Partially Hydrolyzed Poly(acrylamide)/Calcium(II) Complexes. *Macromolecules* **1999**, *32*, 585–589. [CrossRef]
183. Ohmine, I.; Tanaka, T. Salt effects on the phase transition of ionic gels. *J. Chem. Phys.* **1982**, *77*, 5725–5729. [CrossRef]

184. Morris, E.R.; Rees, D.A.; Young, G.; Walkinshaw, M.D.; Darke, A. Order-disorder transition for a bacterial polysaccharide in solution. A role for polysaccharide conformation in recognition between Xanthomonas pathogen and its plant host. *J. Mol. Biol.* **1977**, *110*, 1–16. [CrossRef]
185. Dentini, M.; Crescenzi, V.; Blasi, D. Conformational properties of xanthan derivatives in dilute aqueous solution. *Int. J. Biol. Macromol.* **1984**, *6*, 93–98. [CrossRef]
186. Holzwarth, G. Conformation of the extracellular polysaccharide of Xanthomonas campestris. *Biochemistry* **1976**, *15*, 4333–4339. [CrossRef] [PubMed]
187. Moradi-Araghi, A.; Doe, P.H. Hydrolysis and Precipitation of Polyacrylamides in Hard Brines at Elevated Temperatures. *SPE Reserv. Eng.* **1987**, *2*, 189–198. [CrossRef]
188. Kierulf, C.; Sutherland, I.W. Thermal stability of xanthan preparations. *Carbohydr. Polym.* **1988**, *9*, 185–194. [CrossRef]
189. Sabhapondit, A.; Borthakur, A.; Haque, I. Characterization of acrylamide polymers for enhanced oil recovery. *J. Appl. Polym. Sci.* **2003**, *87*, 1869–1878. [CrossRef]
190. Zhong, C.; Luo, P.; Ye, Z.; Chen, H. Characterization and Solution Properties of a Novel Water-soluble Terpolymer for Enhanced Oil Recovery. *Polym. Bull.* **2009**, *62*, 79–89. [CrossRef]
191. Wu, G.; Yu, L.; Jiang, X. Synthesis and properties of an acrylamide-based polymer for enhanced oil recovery: A preliminary study. *Adv. Polym. Technol.* **2018**, *37*, 2763–2773. [CrossRef]
192. Zhu, Y.Y.; Luo, W.L.; Jian, G.Q.; Wang, C.A.; Hou, Q.F.; Niu, J.L. Development and Performance of Water Soluble Salt-Resistant Polymers for Chemical Flooding. *Adv. Mater. Res.* **2012**, *476-478*, 227–235. [CrossRef]
193. Sabhapondit, A.; Borthakur, A.; Haque, I. Water Soluble Acrylamidomethyl Propane Sulfonate (AMPS) Copolymer as an Enhanced Oil Recovery Chemical. *Energy Fuels* **2003**, *17*, 683–688. [CrossRef]
194. Mothé, C.G.; Correia, D.Z.; de França, F.P.; Riga, A.T. Thermaland rheological study of polysaccharides for enhanced oil recovery. *J. Therm. Anal. Calorim.* **2006**, *85*, 31–36. [CrossRef]
195. Ryles, R.G. Chemical Stability Limits of Water-Soluble Polymers Used in Oil Recovery Processes. *SPE Reserv. Eng.* **1988**, *3*, 23–34. [CrossRef]
196. Bridgewater, J.; Pace, S.; Gardner, G.; Schulz, D. Enhanced Oil Recovery with Hydrophobically Associating Polymers Containing n-vinyl-pyrrolidone Functionality. U.S. Patent 4709759, 1 December 1987.
197. McCormick, C.L.; Nonaka, T.; Johnson, C.B. Water-soluble copolymers: 27. Synthesis and aqueous solution behaviour of associative acrylamideN-alkylacrylamide copolymers. *Polymer* **1988**, *29*, 731–739. [CrossRef]
198. McCormick, C.L.; Middleton, J.C.; Cummins, D.F. Water-soluble copolymers. 37. Synthesis and characterization of responsive hydrophobically modified polyelectrolytes. *Macromolecules* **1992**, *25*, 1201–1206. [CrossRef]
199. Hill, A.; Candau, F.; Selb, J. Properties of hydrophobically associating polyacrylamides: Influence of the method of synthesis. *Macromolecules* **1993**, *26*, 4521–4532. [CrossRef]
200. Dowling, K.C.; Thomas, J.K. A novel micellar synthesis and photophysical characterization of water-soluble acrylamide-styrene block copolymers. *Macromolecules* **1990**, *23*, 1059–1064. [CrossRef]
201. Candau, F.; Selb, J. Hydrophobically-modified polyacrylamides prepared by micellar polymerization1Part of this paper was presented at the conference on 'Associating Polymer', Fontevraud, France, November 1997.1. *Adv. Colloid Interface Sci.* **1999**, *79*, 149–172. [CrossRef]
202. English, R.J.; Laurer, J.H.; Spontak, R.J.; Khan, S.A. Hydrophobically Modified Associative Polymer Solutions: Rheology and Microstructure in the Presence of Nonionic Surfactants. *Ind. Eng. Chem. Res.* **2002**, *41*, 6425–6435. [CrossRef]
203. Feng, Y.; Billon, L.; Grassl, B.; Khoukh, A.; François, J. Hydrophobically associating polyacrylamides and their partially hydrolyzed derivatives prepared by post-modification. 1. Synthesis and characterization. *Polymer* **2002**, *43*, 2055–2064. [CrossRef]
204. Volpert, E.; Selb, J.; Candau, F. Influence of the Hydrophobe Structure on Composition, Microstructure, and Rheology in Associating Polyacrylamides Prepared by Micellar Copolymerization. *Macromolecules* **1996**, *29*, 1452–1463. [CrossRef]
205. Klucker, R.; Candau, F.; Schosseler, F. Transient Behavior of Associating Copolymers in a Shear Flow. *Macromolecules* **1995**, *28*, 6416–6422. [CrossRef]
206. Lara-Ceniceros, A.C.; Rivera-Vallejo, C.; Jiménez-Regalado, E.J. Synthesis, characterization and rheological properties of three different associative polymers obtained by micellar polymerization. *Polym. Bull.* **2007**, *58*, 425–433. [CrossRef]
207. Maia, A.M.S.; Costa, M.; Borsali, R.; Garcia, R.B. Rheological Behavior and Scattering Studies of Acrylamide-Based Copolymer Solutions. In *Macromolecular Symposia*; WILEY-VCH Verlag: Weinheim, Germany, 2005; Volume 229, pp. 217–227. [CrossRef]
208. Xu, B.; Li, L.; Zhang, K.; Macdonald, P.M.; Winnik, M.A.; Jenkins, R.; Bassett, D.; Wolf, D.; Nuyken, O. Synthesis and Characterization of Comb Associative Polymers Based on Poly(ethylene oxide). *Langmuir* **1997**, *13*, 6896–6902. [CrossRef]
209. Alami, E.; Almgren, M.; Brown, W. Interaction of Hydrophobically End-Capped Poly(ethylene oxide) with Nonionic Surfactants in Aqueous Solution. Fluorescence and Light Scattering Studies. *Macromolecules* **1996**, *29*, 5026–5035. [CrossRef]
210. Yekta, A.; Duhamel, J.; Brochard, P.; Adiwidjaja, H.; Winnik, M.A. A fluorescent probe study of micelle-like cluster formation in aqueous solutions of hydrophobically modified poly(ethylene oxide). *Macromolecules* **1993**, *26*, 1829–1836. [CrossRef]
211. Maechling-Strasser, C.; François, J.; Clouet, F.; Tripette, C. Hydrophobically end-capped poly (ethylene oxide) urethanes: 1. Characterization and experimental study of their association in aqueous solution. *Polymer* **1992**, *33*, 627–636. [CrossRef]
212. Yang, X.; Liu, J.; Li, P.; Liu, C. Self-assembly properties of hydrophobically associating perfluorinated polyacrylamide in dilute and semi-dilute solutions. *J. Polym. Res.* **2015**, *22*, 103. [CrossRef]

213. Huang, Z.; Lu, H.; He, Y. Amphoteric hydrophobic associative polymer: I synthesis, solution properties and effect on solution properties of surfactant. *Colloid Polym. Sci.* **2006**, *285*, 365–370. [CrossRef]
214. Gou, S.; Luo, S.; Liu, T.; Zhao, P.; He, Y.; Pan, Q.; Guo, Q. A novel water-soluble hydrophobically associating polyacrylamide based on oleic imidazoline and sulfonate for enhanced oil recovery. *New J. Chem.* **2015**, *39*, 7805–7814. [CrossRef]
215. Shashkina, Y.A.; Zaroslov, Y.D.; Smirnov, V.A.; Philippova, O.E.; Khokhlov, A.R.; Pryakhina, T.A.; Churochkina, N.A. Hydrophobic aggregation in aqueous solutions of hydrophobically modified polyacrylamide in the vicinity of overlap concentration. *Polymer* **2003**, *44*, 2289–2293. [CrossRef]
216. Quan, H.; Li, Z.; Huang, Z. Self-assembly properties of a temperature- and salt-tolerant amphoteric hydrophobically associating polyacrylamide. *RSC Adv.* **2016**, *6*, 49281–49288. [CrossRef]
217. Argillier, J.F.; Audibert, A.; Lecourtier, J.; Moan, M.; Rousseau, L. Solution and adsorption properties of hydrophobically associating water-soluble polyacrylamides. *Colloids Surf. A Physicochem. Eng. Asp.* **1996**, *113*, 247–257. [CrossRef]
218. Grassl, B.; Francois, J.; Billon, L. Associating behaviour of polyacrylamide modified with a new hydrophobic zwitterionic monomer. *Polym. Int.* **2001**, *50*, 1162–1169. [CrossRef]
219. Zhou, H.; Song, G.-Q.; Zhang, Y.-X.; Chen, J.; Jiang, M.; Hogen-Esch, T.E.; Dieing, R.; Ma, L.; Haeussling, L. Hydrophobically Modified Polyelectrolytes, 4. Synthesis and Solution Properties of Fluorocarbon-Containing Poly(acrylic acid). *Macromol. Chem. Phys.* **2001**, *202*, 3057–3064. [CrossRef]
220. Zhong, C.; Huang, R.; Zhang, X.; Dai, H. Synthesis, characterization, and solution properties of an acrylamide-based terpolymer with butyl styrene. *J. Appl. Polym. Sci.* **2007**, *103*, 4027–4038. [CrossRef]
221. Al-Sabagh, A.M.; Kandile, N.G.; El-Ghazawy, R.A.; Noor El-Din, M.R.; El-Sharaky, E.A. Solution properties of hydrophobically modified polyacrylamides and their potential use for polymer flooding application. *Egypt. J. Pet.* **2016**, *25*, 433–444. [CrossRef]
222. Al-Sabagh, A.M.; Kandile, N.G.; El-Ghazawy, R.A.; Noor El-Din, M.R.; El-Sharaky, E.A. Novel Polymerizable Nonionic Surfactants (Surfmers) Corporate with Alkenylsuccinic Anhydride: Synthesis, Surface, and Thermodynamic Properties. *J. Dispers. Sci. Technol.* **2012**, *33*, 1458–1469. [CrossRef]
223. Zhong, C.; Jiang, L.; Peng, X. Synthesis and solution behavior of comb-like terpolymers with poly(ethylene oxide) macromonomer. *J. Polym. Sci. Part A Polym. Chem.* **2010**, *48*, 1241–1250. [CrossRef]
224. Mirzaie Yegane, M.; Hashemi, F.; Vercauteren, F.; Meulendijks, N.; Gharbi, R.; Boukany, P.E.; Zitha, P. Rheological response of a modified polyacrylamide–silica nanoparticles hybrid at high salinity and temperature. *Soft Matter* **2020**, *16*, 10198–10210. [CrossRef]
225. Hourdet, D.; Gadgil, J.; Podhajecka, K.; Badiger, M.V.; Brûlet, A.; Wadgaonkar, P.P. Thermoreversible Behavior of Associating Polymer Solutions: Thermothinning versus Thermothickening. *Macromolecules* **2005**, *38*, 8512–8521. [CrossRef]
226. Bokias, G.; Hourdet, D.; Iliopoulos, I.; Staikos, G.; Audebert, R. Hydrophobic Interactions of Poly(N-isopropylacrylamide) with Hydrophobically Modified Poly(sodium acrylate) in Aqueous Solution. *Macromolecules* **1997**, *30*, 8293–8297. [CrossRef]
227. Hourdet, D.; L'Alloret, F.; Audebert, R. Synthesis of thermoassociative copolymers. *Polymer* **1997**, *38*, 2535–2547. [CrossRef]
228. Bastiat, G.; Grassl, B.; François, J. Study of sodium dodecyl sulfate/poly(propylene oxide) methacrylate mixed micelles for the synthesis of thermo-associative polymers by micellar polymerization. *Polym. Int.* **2002**, *51*, 958–965. [CrossRef]
229. McCormick, C.L.; Johnson, C.B. Water-Soluble Polymers. XXXIV. Ampholyte Terpolymers of Sodium 3-Acrylamido-3-Methylbutanoatewith 2-Acrylamido-2-Methylpropane-Dimethylammonium Chloride and Acrylamide: Synthesis and Absorbency Behavior. *J. Macromol. Sci. Part A-Chem.* **1990**, *27*, 539–547. [CrossRef]
230. Shedge, A.S.; Lele, A.K.; Wadgaonkar, P.P.; Hourdet, D.; Perrin, P.; Chassenieux, C.; Badiger, M.V. Hydrophobically Modified Poly(acrylic acid) Using 3-Pentadecylcyclohexylamine: Synthesis and Rheology. *Macromol. Chem. Phys.* **2005**, *206*, 464–472. [CrossRef]
231. McCormick, C.L.; Salazar, L.C. Water-Soluble Copolymers.46. Hydrophilic Sulfobetaine Copolymers of Acrylamide and 3-(2-Acrylamido-2-Methylpropanedimethyl-Ammonio)-1-Propanesulphonate. *Polymer* **1992**, *33*, 4617–4624. [CrossRef]
232. Xie, X.; Hogen-Esch, T.E. Copolymers of N,N-Dimethylacrylamide and 2-(N-ethylperfluorooctanesulfonamido)ethyl Acrylate in Aqueous Media and in Bulk. Synthesis and Properties. *Macromolecules* **1996**, *29*, 1734–1745. [CrossRef]
233. Rashidi, M. *Physico-Chemistry Characterization of Sulfonated Polyacrylamide Polymers for Use in Polymer Flooding*; The University of Bergen: Bergen, Norway, 2010.
234. Gaillard, N.; Giovannetti, B.; Leblanc, T.; Thomas, A.; Braun, O.; Favero, C. Selection of Customized Polymers to Enhance Oil Recovery from High Temperature Reservoirs. In Proceedings of the SPE Latin American and Caribbean Petroleum Engineering Conference, Quito, Ecuador, 18–20 November 2015; p. 15.
235. Stahl, G.A.; Moradi-Araghi, A.; Doe, P.H. High Temperature and Hardness Stable Copolymers of Vinylpyrrolidone and Acrylamide. In *Water-Soluble Polymers for Petroleum Recovery*; Stahl, G.A., Schulz, D.N., Eds.; Springer: Boston, MA, USA, 1988; pp. 121–130.
236. Peiffer, D.G. Hydrophobically associating polymers and their interactions with rod-like micelles. *Polymer* **1990**, *31*, 2353–2360. [CrossRef]
237. Zhuang, D.-Q.; Ai-hua Da, J.C.; Zhang, Y.-X.; Dieing, R.; Ma, L.; Haeussling, L. Hydrophobically modified polyelectrolytes II: Synthesis and characterization of poly(acrylic acid-co-alkyl acrylate). *Polym. Adv. Technol.* **2001**, *12*, 616–625. [CrossRef]
238. Abu-Sharkh, B.F.; Yahaya, G.O.; Ali, S.A.; Kazi, I.W. Solution and interfacial behavior of hydrophobically modified water-soluble block copolymers of acrylamide and N-phenethylacrylamide. *J. Appl. Polym. Sci.* **2001**, *82*, 467–476. [CrossRef]

239. Wang, Y.; Lu, Z.; Han, Y.; Feng, Y.; Tang, C. A Novel Thermoviscosifying Water-Soluble Polymer for Enhancing Oil Recovery from High-Temperature and High-Salinity Oil Reservoirs. *Adv. Mater. Res.* **2011**, *306–307*, 654–657. [CrossRef]
240. Bataweel, M.A.; Yadhalli Shivaprasad, A.; Nasr-El-Din, H.A. Low-Tension Polymer Flooding Using Amphoteric surfactant in High Salinity/High Hardness and High Temperature Conditions in Sandstone Cores. In Proceedings of the SPE EOR Conference at Oil and Gas West Asia, Muscat, Oman, 16–18 April 2012; p. 23.
241. Wu, Y.; Mahmoudkhani, A.; Watson, P.; Fenderson, T.R.; Nair, M. Development of New Polymers with Better Performance under Conditions of High Temperature and High Salinity. In Proceedings of the SPE EOR Conference at Oil and Gas West Asia, Muscat, Oman, 16–18 April 2012; p. 11.
242. Leblanc, T.; Braun, O.; Thomas, A.; Divers, T.; Gaillard, N.; Favero, C. Rheological Properties of Stimuli-Responsive Polymers in Solution to Improve the Salinity and Temperature Performances of Polymer-Based Chemical Enhanced Oil Recovery Technologies. In Proceedings of the SPE Asia Pacific Enhanced Oil Recovery Conference, Kuala Lumpur, Malaysia, 11–13 August 2015; p. 17.
243. Tavakkoli, O.; Kamyab, H.; Shariati, M.; Mustafa Mohamed, A.; Junin, R. Effect of nanoparticles on the performance of polymer/surfactant flooding for enhanced oil recovery: A review. *Fuel* **2022**, *312*, 122867. [CrossRef]
244. Ogolo, N.A.; Olafuyi, O.A.; Onyekonwu, M.O. Enhanced Oil Recovery Using Nanoparticles. In Proceedings of the SPE Saudi Arabia Section Technical Symposium and Exhibition, Al-Khobar, Saudi Arabia, 8–11 April 2012; p. 9.
245. Miranda, C.R.; Lara, L.S.d.; Tonetto, B.C. Stability and Mobility of Functionalized Silica Nanoparticles for Enhanced Oil Recovery Applications. In Proceedings of the SPE International Oilfield Nanotechnology Conference and Exhibition, Noordwijk, The Netherlands, 12–14 June 2012; p. 11.
246. Wang, L.; Wang, Z.; Yang, H.; Yang, G. The study of thermal stability of the SiO2 powders with high specific surface area. *Mater. Chem. Phys.* **1999**, *57*, 260–263. [CrossRef]
247. Zhao, M.; Zhang, Y.; Chenwei, Z.; Dai, C.; Gao, M.; Li, Y.; Lv, W.; Jiang, J.; Wu, Y. Can More Nanoparticles Induce Larger Viscosities of Nanoparticle-Enhanced Wormlike Micellar System (NEWMS)? *Materials* **2017**, *10*, 1096. [CrossRef]
248. Bera, A.; Belhaj, H. Application of nanotechnology by means of nanoparticles and nanodispersions in oil recovery—A comprehensive review. *J. Nat. Gas Sci. Eng.* **2016**, *34*, 1284–1309. [CrossRef]
249. Hu, Z.; Nourafkan, E.; Gao, H.; Wen, D. Microemulsions stabilized by in-situ synthesized nanoparticles for enhanced oil recovery. *Fuel* **2017**, *210*, 272–281. [CrossRef]
250. Zhu, D.; Wei, L.; Wang, B.; Feng, Y. Aqueous Hybrids of Silica Nanoparticles and Hydrophobically Associating Hydrolyzed Polyacrylamide Used for EOR in High-Temperature and High-Salinity Reservoirs. *Energies* **2014**, *7*, 3858–3871. [CrossRef]
251. Wiśniewska, M.; Terpiłowski, K.; Chibowski, S.; Urban, T.; Zarko, V.I.; Gun'ko, V.M. Effect of polyacrylic acid (PAA) adsorption on stability of mixed alumina-silica oxide suspension. *Powder Technol.* **2013**, *233*, 190–200. [CrossRef]
252. Hu, Z.; Haruna, M.; Gao, H.; Nourafkan, E.; Wen, D. Rheological Properties of Partially Hydrolyzed Polyacrylamide Seeded by Nanoparticles. *Ind. Eng. Chem. Res.* **2017**, *56*, 3456–3463. [CrossRef]
253. Bhardwaj, P.; Singh, S.; Singh, V.; Aggarwal, S.; Mandal, U.K. Nanosize Polyacrylamide/SiO_2 Composites by Inverse Microemulsion Polymerization. *Int. J. Polym. Mater. Polym. Biomater.* **2008**, *57*, 404–416. [CrossRef]
254. Cao, J.; Song, T.; Zhu, Y.; Wang, X.; Wang, S.; Yu, J.; Ba, Y.; Zhang, J. Aqueous hybrids of amino-functionalized nanosilica and acrylamide-based polymer for enhanced oil recovery. *RSC Adv.* **2018**, *8*, 38056–38064. [CrossRef] [PubMed]
255. Petit, L.; Bouteiller, L.; Brûlet, A.; Lafuma, F.; Hourdet, D. Responsive Hybrid Self-Assemblies in Aqueous Media. *Langmuir* **2007**, *23*, 147–158. [CrossRef] [PubMed]
256. Portehault, D.; Petit, L.; Pantoustier, N.; Ducouret, G.; Lafuma, F.; Hourdet, D. Hybrid thickeners in aqueous media. *Colloids Surf. A Physicochem. Eng. Asp.* **2006**, *278*, 26–32. [CrossRef]
257. Hourdet, D.; Petit, L. Hybrid Hydrogels: Macromolecular Assemblies through Inorganic Cross-Linkers. *Macromol. Symp.* **2010**, *291–292*, 144–158. [CrossRef]
258. Lin, W.-C.; Fan, W.; Marcellan, A.; Hourdet, D.; Creton, C. Large Strain and Fracture Properties of Poly(dimethylacrylamide)/Silica Hybrid Hydrogels. *Macromolecules* **2010**, *43*, 2554–2563. [CrossRef]
259. Maghzi, A.; Kharrat, R.; Mohebbi, A.; Ghazanfari, M.H. The impact of silica nanoparticles on the performance of polymer solution in presence of salts in polymer flooding for heavy oil recovery. *Fuel* **2014**, *123*, 123–132. [CrossRef]
260. Schottner, G. Hybrid Sol−Gel-Derived Polymers: Applications of Multifunctional Materials. *Chem. Mater.* **2001**, *13*, 3422–3435. [CrossRef]
261. Gao, C.; Shi, J.; Zhao, F. Successful polymer flooding and surfactant-polymer flooding projects at Shengli Oilfield from 1992 to 2012. *J. Pet. Explor. Prod. Technol.* **2014**, *4*, 1–8. [CrossRef]
262. Saleh, L.; Wei, M.; Bai, B. Data Analysis and Novel Screening Criteria for Polymer Flooding Based on a Comprehensive Database. In Proceedings of the SPE Improved Oil Recovery Symposium, Tulsa, OK, USA, 12–16 April 2014; p. 18.
263. Morel, D.C.; Vert, M.; Jouenne, S.; Gauchet, R.; Bouger, Y. First Polymer Injection in Deep Offshore Field Angola: Recent Advances in the Dalia/Camelia Field Case. *Oil Gas Facil.* **2012**, *1*, 43–52. [CrossRef]
264. Morel, D.C.; Jouenne, S.; Vert, M.; Nahas, E. Polymer Injection in Deep Offshore Field: The Dalia Angola Case. In Proceedings of the SPE Annual Technical Conference and Exhibition, Denver, CO, USA, 21–24 September 2008; p. 12.
265. Song, K.; Tao, J.; Lyu, X.; Xu, Y.; Liu, S.; Wang, Z.; Liu, H.; Zhang, Y.; Fu, H.; Meng, E.; et al. Recent Advances in Polymer Flooding in China. *Molecules* **2022**, *27*, 6978. [CrossRef]

266. Zhang, Y.; Feng, Y.; Li, B.; Han, P. Enhancing oil recovery from low-permeability reservoirs with a self-adaptive polymer: A proof-of-concept study. *Fuel* **2019**, *251*, 136–146. [CrossRef]
267. Zhu, R.; Feng, Y.; Luo, P. Net Contribution of Hydrophobic Association to the Thickening Power of Hydrophobically Modified Polyelectrolytes Prepared by Micellar Polymerization. *Macromolecules* **2020**, *53*, 1326–1337. [CrossRef]
268. Leonhardt, B.; Santa, M.; Steigerwald, A.; Kaeppler, T. *Polymer Flooding with the Polysaccharide Schizophyllan—First Field Trial Results*; European Association of Geoscientists & Engineers: Bunnik, The Netherlands, 2013. [CrossRef]
269. Prasad, D.; Ernst, B.; Incera, G.; Leonhardt, B.; Reimann, S.; Mahler, E.; Zarfl, M. *Field Testing the Polysaccharide Schizophyllan—Single Well Test Design and Current Results*; European Association of Geoscientists & Engineers: Bunnik, The Netherlands, 2017.
270. Jouenne, S. Polymer flooding in high temperature, high salinity conditions: Selection of polymer type and polymer chemistry, thermal stability. *J. Pet. Sci. Eng.* **2020**, *195*, 107545. [CrossRef]
271. Wassmuth, F.R.; Green, K.; Arnold, W.; Cameron, N. Polymer Flood Application to Improve Heavy Oil Recovery at East Bodo. *J. Can. Pet. Technol.* **2009**, *48*, 55–61. [CrossRef]
272. Delamaide, E. Review of Canadian Field Cases of Chemical Floods with Associative Polymer. In Proceedings of the SPE Improved Oil Recovery Conference, 31 August–4 September 2020.
273. Delamaide, E.; Zaitoun, A.; Renard, G.; Tabary, R. Pelican Lake Field: First Successful Application of Polymer Flooding In a Heavy-Oil Reservoir. *SPE Reserv. Eval. Eng.* **2014**, *17*, 340–354. [CrossRef]
274. Zhou, W.; Zhang, J.; Han, M.; Xiang, W.; Feng, G.; Jiang, W. Application of Hydrophobically Associating Water-soluble Polymer for Polymer Flooding in China Offshore Heavy Oilfield. In Proceedings of the International Petroleum Technology Conference, Dubai, United Arab Emirates, 17–19 December 2007; p. 5.
275. Demin, W.; Zhang, Z.; Chun, L.; Cheng, J.; Du, X.; Li, Q. A Pilot for Polymer Flooding of Saertu Formation S II 10-16 in the North of Daqing Oil Field. In Proceedings of the SPE Asia Pacific Oil and Gas Conference, Adelaide, Australia, 28–31 October 2020; p. 11.
276. Liu, B.; Sun, X.S.; Wang, K.; Xu, H.; Liu, Q.; Liu, X.; Song, S. Flooded by High Concentration Polymer Doubled Oil Recovery of Common Polymer on Field Test with 20% Closed to the Result of Lab Test in Daqing. In Proceedings of the International Oil Conference and Exhibition in Mexico, Veracruz, Mexico, 27–30 June 2007; p. 9.
277. Kang, X.; Zhang, J.; Sun, F.; Zhang, F.; Feng, G.; Yang, J.; Zhang, X.; Xiang, W. A Review of Polymer EOR on Offshore Heavy Oil Field in Bohai Bay, China. In Proceedings of the SPE Enhanced Oil Recovery Conference, Kuala Lumpur, Malaysia, 19–20 July 2011. [CrossRef]
278. Guo, Y.; Zhang, J.; Liu, Y.; Liu, G.; Xue, X.; Luo, P.; Ye, Z.; Zhang, X.; Liang, Y. Successful Scale Application of Associative Polymer Flooding for Offshore Heavy Oilfield in Bohai Bay of China. In Proceedings of the SPE/IATMI Asia Pacific Oil & Gas Conference and Exhibition, 29–31 October 2019.
279. He, J.; Song, Z.; Qiu, L.; Xie, F.; Tan, Z.; Yue, Q.; Li, X. High Temperature Polymer Flooding in Thick Reservoir in ShuangHe Oilfield. In Proceedings of the SPE International Oil and Gas Conference and Exhibition in China, Beijing, China, 2–6 November 1998; p. 11.
280. de Melo, M.A.; Holleben, C.R.; Silva, I.G.; de Barros Correia, A.; Silva, G.A.; Rosa, A.J.; Lins, A.G., Jr.; de Lima, J.C. Evaluation of Polymer-Injection Projects in Brazil. In Proceedings of the SPE Latin American and Caribbean Petroleum Engineering Conference, Rio de Janeiro, Brazil, 20–23 June 2005; p. 17.
281. de Melo, M.A.; da Silva, I.P.G.; de Godoy, G.M.R.; Sanmartim, A.N. Polymer Injection Projects in Brazil: Dimensioning, Field Application and Evaluation. In Proceedings of the SPE/DOE Improved Oil Recovery Symposium, Tulsa, OK, USA, 13–17 April 2002; p. 11.
282. Al-saadi, F.S.; Al-amri, B.A.; Al Nofli, S.M.; Van Wunnik, J.N.M.; Jaspers, H.F.; Al Harthi, S.; Shuaili, K.; Cherukupalli, P.K.; Chakravarthi, R. Polymer Flooding in a Large Field in South Oman—Initial Results and Future Plans. In Proceedings of the SPE EOR Conference at Oil and Gas West Asia, Muscat, Oman, 16–18 April 2012; p. 7.
283. Koning, E.J.L.; Mentzer, E.; Heemskerk, J. Evaluation of a Pilot Polymer Flood in the Marmul Field, Oman. In Proceedings of the SPE Annual Technical Conference and Exhibition, Houston, TX, USA, 2–5 October1988; p. 9.
284. Moe Soe Let, K.P.; Manichand, R.N.; Seright, R.S. Polymer Flooding a ~500-cp Oil. In Proceedings of the SPE Improved Oil Recovery Symposium, Tulsa, OK, USA, 14–18 April 2012; p. 13.
285. Kumar, P.; Raj, R.; Koduru, N.; Kumar, S.; Pandey, A. Field Implementation of Mangala Polymer Flood: Initial Challenges, Mitigation and Management. In Proceedings of the SPE EOR Conference at Oil and Gas West Asia, Muscat, Oman, 21–23 March 2016; p. 20.
286. Mehta, N.; Kapadia, G.; Selvam, V. Challenges in Full Field Polymer Injection Mangala in Field. In Proceedings of the SPE EOR Conference at Oil and Gas West Asia, Muscat, Oman, 21–23 March 2016.